CONTEXTUALITY AND NON-LOCALITY RELATIONS IN QUANTUM SYSTEMS

by
FIRAT DİKER

Submitted to the Graduate School of Engineering and Natural Sciences
in partial fulfilment of
the requirements for the degree of Doctor of Philosophy

Sabancı University
December 2022

ABSTRACT

CONTEXTUALITY AND NON-LOCALITY RELATIONS IN QUANTUM SYSTEMS

FIRAT DİKER

PHYSICS Ph.D. DISSERTATION, DECEMBER 2022

Dissertation Supervisor: Prof. Mehmet Zafer Gedik

Keywords: Contextuality, Non-locality, Entanglement, Quantum Measurement, Concurrence, Delayed-choice, the wave-particle duality

Quantum contextuality is the concept that the outcome of a measurement on a system is not always independent of other measurements performed simultaneously on the system. The simplest example where we observe quantum contextuality is the Klyachko-Can-Binicioğlu-Shumovsky (KCBS) measurement scenario which includes a five-measurement state-dependent non-contextuality inequality violated by some qutrit states. We have approached the KCBS inequality from three different perspectives which form the main components of this thesis: (1) We have looked into the symmetries of the KCBS pentagram, i.e., the conservation of quantum contextuality under rotations in the physical space. We work with the quantum systems belonging to the real subgroup of the three-dimensional Hilbert space. We provide the data on Euler rotation angles for maximal quantum contextuality. By using the data, we have found mathematical relations between rotation angles and qutrit states parameterized with spherical coordinates; (2) In the second part of my thesis, we have found the relation between quantum contextuality and concurrence (a measure of entanglement) in the KCBS measurement scenario. We have also found the degree of quantum contextuality for a given concurrence when the KCBS measurements are performed. Using this relation, we have made a comparison between the maximal violations of the classical inequalities (the Bell and KCBS inequalities) for any degree of entanglement. Moreover, we have calculated the degree of violation when maximal entanglement or non-entanglement is observed. We have found a new lower bound for the non-entangled states in the KCBS scenario; (3) After

discussing the different versions of the quantum delayed-choice experiment, we have introduced a quantum circuit that corresponds to a modified version of the same experiment where one sees that quantum contextuality and entanglement are well correlated with wave and particle properties of a quantum state. This shows that quantum contextuality is in good agreement with the wave-particle duality.

ÖZET

KUANTUM SİSTEMLERİNDE BAĞLAMSALLIK VE YEREL OLMAMA İLİŞKİLERİ

FIRAT DİKER

FİZİK DOKTORA TEZİ, ARALIK 2022

Tez Danışmanı: Prof. Dr. Mehmet Zafer Gedik

Anahtar Kelimeler: Bağlamsallık, Yerel olmama, Dolaşıklık, Kuantum ölçümü, Uyum, Ertelemeli seçim, dalga-parçacık ikililiği

Kuantum bağlamsallık, bir ölçümün sonucunun birlikte gerçekleştirilen diğer ölçümlerden bağımsız olmadığını ifade eden kavramdır. Kuantum bağlamsallığını gözlemlediğimiz en basit örnek, bazı qutrit durumları tarafından ihlal edilen beş ölçümlü duruma bağlı bağlamsal olmayan eşitsizliği içeren Klyachko-Can-Binicioğlu-Shumovsky (KCBS) ölçüm senaryosudur. KCBS eşitsizliğine, bu tezin ana bileşenlerini oluşturan üç farklı açıdan yaklaştık: (1) KCBS pentagramının simetrilerini, yani fiziksel Öklid uzayı $\mathbb{E}^3$'daki dönmeler altında kuantum bağlamsallığının korunmasını inceledik. Üç boyutlu Hilbert uzayının gerçek alt grubuna ait kuantum sistemleriyle çalıştık. Maksimum kuantum bağlamsallığı için Euler dönüş açılarına ilişkin verileri sağlıyoruz. Verileri kullanarak, küresel koordinatlarla parametrelenmiş qutrit durumları ile dönme açıları arasında matematiksel ilişkiler bulduk; (2) Tezimin ikinci bölümünde, KCBS ölçüm senaryosunda kuantum bağlamsallık ile uyum (dolaşıklık ölçütü) arasındaki ilişkiyi bulduk. Ayrıca, KCBS ölçümleri yapıldığında belirli bir uyum için kuantum bağlamsallık derecesini de bulduk. Bu ilişkiyi kullanarak, keyfi bir dolaşıklık için KCBS ve Bell eşitsizliklerinin maksimum ihlalleri arasında karşılaştırma yaptık. Ayrıca, maksimum dolaşıklık veya dolaşıklık olmama gözlemlendiğinde ihlal derecesini hesapladık. KCBS senaryosundaki dolaşık olmayan durumlar için yeni bir alt sınır bulduk; (3) Kuantum ertelemeli seçim deneyinin farklı versiyonlarından bahsettikten sonra aynı deneyin modifiye edilmiş haline karşılık gelen ve kuantum bağlamsallık ile dolaşıklığın parçacığa ait dalga ve parçacık özellikleriyle ilintili olduğu görülen bir kuantum devresi sunduk. Bu bize kuantum bağlamsallığın

dalga-parçacık ikililiğiyle uyum içerisinde olduğunu gösterdi.

ACKNOWLEDGEMENTS

I want to thank my supervisor Prof. Mehmet Zafer Gedik for his guidance and support throughout my studies. I am thankful to him for putting his faith in me.

Prof. İnanç Adagideli and Prof. Özgür Erçetin helped me during my thesis progress through their useful discussions. I want to express my appreciation to them.

I want to thank Ali Can Günhan and Daniel Lee Calvey for providing language help.

Another person I am grateful to is Prof. Metin Arık. He is not only a teacher for me but also a close acquaintance. He guided me during my master's and showed intimacy when I worked with him before I came to Sabanci University. His knowledge of fundamental concepts of physics helped me improve my knowledge. For that, I am deeply thankful to him.

I acknowledge the support and full scholarship from Sabanci University.

Completing this dissertation has been a long and painful process, and I cannot thank my family enough for their emotional support throughout this journey. My parents, Müzeyyen and Duran, taught me how to think independently and raised me to the person I am now, and I am proud to be their son. My older brother Okan has always been ready to help me, and I will never forget that he taught me how to ride a bicycle when we were kids. I believe my father, Duran Diker, who passed away in 2019 summer, is watching me from heaven and will see me finally graduate.

Finally, I owe a special thanks to my wife, Aysel Arslan. She has been my source of power with her presence throughout the ups and downs of my Ph.D. journey. Her love, patience, and support were the biggest driving force behind me in completing this dissertation.

Bu çalışmayı, 2019 yılında kaybettiğim ve hayattayken maddi manevi her türlü desteğini benden esirgemeyen çok sevgili babam Duran Diker'e ithaf ediyorum.

TABLE OF CONTENTS

LIST OF TABLES

LIST OF FIGURES

LIST OF ABBREVIATONS

1.   INTRODUCTION

The quantum revolution has changed our understanding of the microscopic world and took place at the beginning of the twentieth century. It is unprecedented in human history. Not only did we see the failure of the rules of classical physics on a small scale, but we found a better explanation that is far broader in scope and far richer regarding applicability.

The pioneering works of quantum mechanics are de Broglie's matter waves, the Einstein-Debye theory of specific heats, Planck's radiation law, the Bohr atom, and some key experiments such as the Davisson-Germer-Thompson experiment, the Compton effect, and the Franck-Hertz experiment. These made the physicists abandon the classical description of matter and energy for small-scale interactions. Finally, this led to the formulation of quantum mechanics.

For our survival, we make assumptions about nature and try to formulate them to predict what may occur. Then, we test our predictions. These tests, namely, scientific experiments, may or may not agree with our predictions. Depending on the results of these experiments, we make physical laws about nature that thoroughly accommodate quantum-mechanical observations. We will mainly follow the method given in Sakurai's textbook to discuss the basic subjects (Sakurai & Napolitano, 2011).

1.1 The Stern-Gerlach Experiment

We will discuss the Stem-Gerlach experiment in the first section. First, we heat silver (Ag) atoms in an oven with a small hole. We see that some of the silver atoms escape through that hole, and the beam affected by an inhomogeneous magnetic field after it goes through a collimator. A pair of pole pieces produce the magnetic

field, and one of the pieces has a very sharp edge.

We must answer the following question: What is the result when we apply the magnetic field on the silver atoms? The silver atom is made up of 47 electrons and a nucleus. 46 out of the 47 electrons are distributed in a spherically symmetrical electron cloud and do not have net angular momentum. We observe that the atom does have an angular momentum because of the spin-intrinsic as opposed to the last electron's orbital momentum. The atom's magnetic moment is equal to the 47th electron's spin magnetic moment, which means $\mu \propto \boldsymbol{S}$ (μ is the magnetic moment of the atom, $\boldsymbol{S}$ is the electron spin).

The interaction between the external magnetic field and the atom is due to its magnetic moment:

$$(1.1) \qquad\qquad E_I = -\boldsymbol{\mu} \cdot \boldsymbol{B},$$

and the z-component of the force exerted on the atom is as follows:

$$(1.2) \qquad\qquad F_z = \frac{\partial}{\partial z}(\boldsymbol{\mu} \cdot \boldsymbol{B}) \simeq \mu_z \frac{\partial B_z}{\partial z}.$$

We can ignore the components of the magnetic field in other directions. Because the atom is too heavy, the classical concept of trajectory can be used.

When $\mu_z > 0$ ($S_z < 0$), a downward force is exerted on the atom. While the $\mu_z < 0$ ($S_z > 0$), there is an upward force. The beam gets split depending on the values of μ_z. In other words, in the Stern-Gerlach (SG) experiment, we measure $\boldsymbol{\mu}$ and $\boldsymbol{S}$ along the z-axis. The orientation of the atoms in the oven is random. We do not try to select a specific direction for the orientation of $\boldsymbol{\mu}$. If the electrons behaved like classical particles, we would measure all values of μ_z between $|\boldsymbol{\mu}|$ and -$|\boldsymbol{\mu}|$. We would observe the beams coming from the SG apparatus on the expected range. Instead, we see that there are only two "spots" where we observe the atoms, corresponding to "up" and "down" states. In other words, the silver beam is splitted by the SG apparatus, and beams fall on two spots after splitting. This fact is called "space quantization" when observed for the first time.

Only two values of the z-component of $\boldsymbol{S}$ are measured: up and down, which we denote by S_z+ and S_z-. These are shown below:

$$(1.3) \qquad\qquad S_z^{\pm} = \pm\hbar/2,$$

where

$$\hbar = 1.0546 \times 10^{-27} erg - s$$

$$= 6.5822 \times 10^{-16} eV - s$$

Observing the electron spin angular momentum is one of the pioneering works shaping quantum physics.

According to the classical description of particles, the atoms would have been observed over a vertical distance and distributed continuously. Instead, what we observe contradicts classical physics. The beam interestingly divides into two parts (up and down).

One may apply an inhomogeneous field in different directions. For example, a field is applied in the x-direction, and the beam proceeds in the y-direction. In this case, the beam can be divided into S_x+ and S_x- components.

1.2 Spin-1/2 States

In this section, the spin-1/2 systems will be discussed. We use the base kets, $|Sz;\pm\rangle$ denoted by $|\pm\rangle$ for brevity. For these base kets, the identity operator is written as

(1.5) $$I = |+\rangle\langle+| + |-\rangle\langle-|.$$

We can write S_z as

(1.6) $$S_z = (\hbar/2)(|+\rangle\langle+| - |-\rangle\langle-|)$$

which gives

(1.7) $$S_z|\pm\rangle = \pm\hbar/2|\pm\rangle.$$

There are two other operators which flip the spin of a particle by also adding the constant $\hbar$ as a coefficient,

(1.8) $$S_+ = \hbar|+\rangle\langle-|, \quad S_- = \hbar|-\rangle\langle+|.$$

If S_+ acts on the spin-up ket, it turns into a null ket. This is also the case when S_- acts on the spin-down ket. S_+ raises the spin by one unit of $\hbar$. 2. It is impossible to have a spin-3/2 particle out of a spin-1/2 particle, so we get a null state when S_+ acts on the spin-up state or S_- is applied to the spin-down state. 1. The matrix representations of the spin states in S_z basis are in the following:

$$(1.9) \qquad |+\rangle = \begin{pmatrix} 1 \\ 0 \end{pmatrix}, \quad |-\rangle = \begin{pmatrix} 0 \\ 1 \end{pmatrix}.$$

The spin operator S_z is given as:

$$(1.10) \qquad S_z = \frac{\hbar}{2} \begin{pmatrix} 1 & 0 \\ 0 & -1 \end{pmatrix},$$

and the raising and lowering operators are

$$(1.11) \qquad S_+ = \hbar \begin{pmatrix} 0 & 1 \\ 0 & 0 \end{pmatrix}, \quad S_- = \hbar \begin{pmatrix} 0 & 0 \\ 1 & 0 \end{pmatrix}.$$

1.2.1 Pauli Two-Component Formalism

Calculations with the states of spin-1/2 systems can be done in the spinor formalism used by Pauli in 1926 for the first time. We can represent a ket (or a bra) in a column (row) matrix. One needs to arrange the expansion coefficients so that any state can be defined using the new base kets. The eigenstates of the S_z matrix are

$$(1.12) \qquad |+\rangle = \begin{pmatrix} 1 \\ 0 \end{pmatrix}, |-\rangle = \begin{pmatrix} 0 \\ 1 \end{pmatrix},$$

which may be shown in rows as well,

$$(1.13) \qquad \langle +| = (1,0), \langle -| = (0,1).$$

Any state can be expressed using these base kets,

$$(1.14) \qquad |\alpha\rangle = |+\rangle\langle +|\alpha\rangle + |-\rangle\langle -|\alpha\rangle = \begin{pmatrix} \langle +|\alpha\rangle \\ \langle -|\alpha\rangle \end{pmatrix}.$$

We may denote $\langle\pm|\alpha\rangle$ as $c_\pm$ which can be complex or real numbers. The matrix elements $\langle\pm|\,S_i\,|\pm\rangle$ give 2×2 matrices where $i=x,y,z$ showing the physical dimensions. These are called *the Pauli matrices*. The matrix representations of *the Pauli matrices* are in the following:

$$(1.15) \qquad S_x = \frac{\hbar}{2}\begin{pmatrix} 0 & 1 \\ 1 & 0 \end{pmatrix}, S_y = \frac{\hbar}{2}\begin{pmatrix} 0 & -i \\ i & 0 \end{pmatrix}, S_z = \frac{\hbar}{2}\begin{pmatrix} 1 & 0 \\ 0 & -1 \end{pmatrix}.$$

One may prefer to express *the Pauli matrices* without $\frac{\hbar}{2}$. We wrote them with the $\frac{\hbar}{2}$ constant. In the literature, *the Pauli matrices* are shown with σ_k when the $\hbar$ constant is omitted. For simplicity, we will use the version without the constant from now on.

1.3 Spin-1 Systems

Pauli spin matrices represent the spin-1/2 particles' spin measurements. In this section, we discuss bosonic states' spin operators which are called spin-1 measurement operators. These operators are 3×3 matrices shown as

$$(1.16) \qquad S_x = \frac{1}{\sqrt{2}}\begin{pmatrix} 0 & 1 & 0 \\ 1 & 0 & 1 \\ 0 & 1 & 0 \end{pmatrix}, S_y = \frac{1}{\sqrt{2}i}\begin{pmatrix} 0 & 1 & 0 \\ -1 & 0 & 1 \\ 0 & -1 & 0 \end{pmatrix},$$

and

$$(1.17) \qquad S_z = \begin{pmatrix} 1 & 0 & 0 \\ 0 & 0 & 0 \\ 0 & 0 & -1 \end{pmatrix}.$$

The spin measurement operator along the z-axis is the matrix that we use for the Klyachko-Can-Binicioğlu-Shumovsky (KCBS) scenario. The eigenkets of S_z are

$$(1.18) \qquad |1\rangle = \begin{pmatrix} 1 \\ 0 \\ 0 \end{pmatrix}, \quad |0\rangle = \begin{pmatrix} 0 \\ 1 \\ 0 \end{pmatrix}, \quad \text{and} \quad |-1\rangle = \begin{pmatrix} 0 \\ 0 \\ 1 \end{pmatrix}.$$

Their eigenvalues are 1, 0 and -1, respectively. The mathematical framework of spin-1/2 and spin-1 particles are very similar. We do not need to discuss the spin-1

matrices since they will often be used when we consider the KCBS scenario.

1.4 Quantum Measurements

We will now discuss quantum measurements which have a crucial role in our work. P. A. M. Dirac defines the measurement process in Quantum Theory as being different from classical measurements (Dirac, 1958):

> A measurement always causes the system to jump into an eigenstate of the dynamical variable that is being measured.

The interpretation of this is as follows: Before we measure observable A, the system is assumed to be in the state

$$(1.19) \qquad |\alpha\rangle = \sum_{a'} c_{a'} |a'\rangle = \sum_{a'} |a'\rangle \langle a'|\alpha\rangle.$$

After the measurement, the system collapses into one of the eigenstates. We may show the process as follows:

$$(1.20) \qquad |\alpha\rangle \to |a'\rangle.$$

The observation affects the measurement, changing the initial state. The observed state is different than it was just before the measurement, in general, if it was not in one of the eigenstates of the measured quantity.

We can not know for 100 percent what we will observe as a result of a measurement. However, we may calculate the probability of finding the state $|a'\rangle$,

$$(1.21) \qquad P_{a'} = \left| \langle a'|\alpha\rangle \right|^2.$$

Note that $|\alpha\rangle$ is normalized,

$$(1.22) \qquad \sum_{a'} P_{a'} = 1.$$

For a collection of identical physical systems, we need to consider a large number of

measurements. Such a collection is called a pure ensemble.

If the state ket is $|a'\rangle$, then the probability of getting a' in A measurement is 1, which is the expected result. When we measure once again, we only get a'. This is the only result we obtain regardless of how many times we perform a measurement. The probability of getting a'' where $a'' \neq a'$ is zero. This is the orthogonality condition between kets. When a particle is in the state $|S_z; +\rangle$, one may certainly say that it is not in the state $|S_z; -\rangle$.

The probability of observing any a' is nonnegative. Furthermore, the sum of probabilities for all a's must be one. This is expressed in Equation 1.22.

The expectation value of an observable A is

$$(1.23) \qquad\qquad \langle A \rangle = \langle \alpha | A | \alpha \rangle$$

which can be rewritten as

$$
\begin{aligned}
\langle A \rangle &= \sum_{a'} \sum_{a''} \langle \alpha | a'' \rangle \langle a'' | A | a' \rangle \langle a' | \alpha \rangle \\
&= \sum_{a'} a' \langle \alpha | a' \rangle \langle a' | \alpha \rangle \\
&= \sum_{a'} a' \left| \langle \alpha | a' \rangle \right|^2 = \sum_{a'} a' P(a').
\end{aligned}
$$

(1.24)

We know well that this is the average of some statistical quantity. One should notice that eigenvalues are not identical to expectation values. For example, $\langle S_z \rangle$ can be any real number between $-\hbar/2$ and $\hbar/2$; in other words, the eigenvalues are the bounds for the average value.

To understand the meaning of measurements better, we will discuss the notion of selective measurement. Previously, we mentioned the Stern-Gerlach experiment where we only observe one of the spin states, and the other state is completely blocked. This is a measurement process performed by a device that lets only one eigenket pass through. This is a selective measurement. Mathematically, we express this as a projection operator,

$$(1.25) \qquad\qquad \Lambda_{a'} = |a'\rangle \langle a'|.$$

1.5 Compatible Observables

In this section, we will discuss the compatibility of observables. The compatibility of the observables A and B are valid when they commute,

(1.26)
$$[A, B] = 0.$$

If they are not compatible, they do not commute,

(1.27)
$$[A, B] \neq 0.$$

For example, $\boldsymbol{S}^2$ and S_z commute, so they are compatible; however, S_x and S_z do not commute and hence are incompatible observables.

We need to introduce the concept of degeneracy. If some eigenkets of an observable have the same eigenvalue, we say there is degeneracy in a quantum system. This causes a problem with labeling each state since, for example, if two eigenkets have the eigenvalue a', we can not use the notation $|a'\rangle$ for labeling. We said earlier that the ket space is spanned by $|a'\rangle$; however, when the number of dimensions is larger than the number of distinct eigenvalues of the observable A, the spanning of the ket space runs into difficulty. When a quantum system has degenerate states for observable A, we may use the eigenvalues of some other observable to define the degenerate states.

Theorem 1.1 *Suppose that $[A, B] = 0$, and there is no degeneracy among the eigenvalues of A. The matrix elements $(\langle a''|\, B \,|a'\rangle)$ are diagonal, and if we use $|a'\rangle$ as the base kets, the matrix elements of A are diagonal as well.*

Due to the compatibility of observables, we see that

(1.28)
$$\left\langle a''\middle|[A, B]\middle|a'\right\rangle = (a'' - a')\left\langle a''\middle|B\middle|a'\right\rangle = 0.$$

So, $\langle a''|\,B\,|a'\rangle$ is equal to zero if $a' \neq a''$.

The matrix elements of B can be written as

(1.29)
$$\left\langle a''\middle|B\middle|a'\right\rangle = \delta_{a'a''}\left\langle a'\middle|B\middle|a'\right\rangle$$

We can represent both observables A and B as diagonal matrices having the same base kets. The observable B can be written as the following matrix:

(1.30)
$$B = \sum_{a''}\middle|a''\right\rangle\left\langle a''\middle|B\middle|a''\right\rangle\left\langle a''\middle|$$

When this operator is applied to an eigenstate of A,

$$B\left|a'\right\rangle = \sum_{a''}\left|a''\right\rangle\left\langle a''\right|B\left|a''\right\rangle\left\langle a''\middle|a'\right\rangle$$

(1.31)
$$= \sum_{a''}\left|a''\right\rangle\left\langle a''\right|B\left|a''\right\rangle\delta_{a'a''}$$

$$= \left|a'\right\rangle\left\langle a'\right|B\left|a'\right\rangle.$$

This is the eigenvalue equation for the observable B with eigenvalue

(1.32)
$$b' = \left\langle a'\right|B\left|a'\right\rangle.$$

The state $\left|a'\right\rangle$ is an eigenket of both A and B operators. We may denote this state as $\left|a',b'\right\rangle$.

The compatible observables have the same eigenkets, denoted by $\left|a',b'\right\rangle$, and have the property

(1.33)
$$A\left|a',b'\right\rangle = a'\left|a',b'\right\rangle,$$

(1.34)
$$B\left|a',b'\right\rangle = b'\left|a',b'\right\rangle.$$

For degenerate systems, the notation $\left|a',b'\right\rangle$ is much more useful. The eigenvalues of L_z (the z-component of orbital angular momentum) and $\boldsymbol{L}^2$ (orbital angular momentum squared) are $m_l\hbar$ and $\hbar^2 l(l+1)$, respectively. $m_z = -l, -l+1, \ldots, +l$ and l is an integer. To express an orbital angular-momentum state specifically, we must specify l and m_z. For example, if $l = 2$, the m_z value can be 0, +2, +1, −1, or −2; if $m_z = 2$, l can be 2, 3, 4, 5, and so on. We can clearly express the orbital angular-momentum state by specifying both quantities. K' is often used to denote (a',b'),

(1.35)
$$\left|K'\right\rangle = \left|a',b'\right\rangle.$$

One may generalize to a case with several compatible observables, namely,

(1.36)
$$[A,B] = [B,C] = [A,C] = ... = 0.$$

Let us assume that there are a set of commuting observables; that is, one may not add any more operators in our case. The commutation relations are given in

9

1.36. There may be degeneracies for each operator, but if we specifically give a combination $(a', b', c', ...)$, then the common eigenket of A, B, C, . . . is expressed clearly. One may again use K' to denote $(a', b', c', ...)$. The orthonormality relation is given for

$$（1.37) \qquad \left| K' \right\rangle = \left| a', b', c', ... \right\rangle$$

as in the following:

$$（1.38) \qquad \left\langle K'' \middle| K' \right\rangle = \delta_{K'K''} = \delta_{a'a''} \delta_{b'b''} \delta_{c'c''}...$$

We can write the completeness relation as

$$（1.39) \qquad \sum_{K'} \left| K' \right\rangle \left\langle K' \right| = \sum_{a'} \sum_{b'} \sum_{c'} ... \left| a', b', c', ... \right\rangle \left\langle a', b', c', ... \right| = 1.$$

Suppose that A and B are compatible observables. One measures the observable A first, and we obtain a'. Subsequently, we may apply the operator B, and as a result, we may obtain b'. Then we measure A again. We always obtain a' as the third result with certainty; that is, the measurement of the observable B does not delete the information obtained in the first measurement of the operator A. The measurement process is as follows:

$$（1.40) \quad \left| \alpha \right\rangle \xrightarrow{A \quad measurement} \left| a', b' \right\rangle \xrightarrow{B \quad measurement} \left| a', b' \right\rangle \xrightarrow{A \quad measurement} \left| a', b' \right\rangle.$$

For the degenerate case, this is what happens: After the first measurement of the observable A, yielding a', the system collapses into some linear combination

$$（1.41) \qquad \sum_{i}^{n} c_{a'}^{(i)} \left| a', b^{(i)} \right\rangle.$$

We get the same eigenvalue a' when the operator A acts on the set of the kets $\left| a', b^{(i)} \right\rangle$. n is the degree of degeneracy. When the operator B acts on the state, one of the terms in the linear combination may be selected. The third measurement of the operator A gives a' as a result. Regardless of degeneracy, A and B measurements do not affect each other. This is called compatibility of the observables A and B.

1.6 Incompatible Observables

In this section, we will discuss incompatible observables. We must point out that incompatible observables have a partial set of the same eigenstates for different operators. If we assume that the previous statement is false, we would have a set of the same eigenkets in accordance with Equations 1.33 and 1.34. One can easily see that

$$(1.42) \qquad AB\left|a',b'\right\rangle = Ab'\left|a',b'\right\rangle = a'b'\left|a',b'\right\rangle,$$

and

$$(1.43) \qquad BA\left|a',b'\right\rangle = Ba'\left|a',b'\right\rangle = a'b'\left|a',b'\right\rangle.$$

This leads to the commutation relation between the observables A and B,

$$(1.44) \qquad [A,B]\left|a',b'\right\rangle = 0.$$

$\left|a',b'\right\rangle$ is not valid for incompatible observables; however, there is an example to be discussed. There may exist a subspace of the ket space such that 1.44 is true for the operators A and B with incompatibility between them. The example is as follows: For an $l = 0$ state, even though L_x and L_z are not compatible, this state is an eigenstate of both L_z and L_x (eigenvalue is zero).

Let us look at an example of selective measurements. There are filters (A), (B), and (C), all of which select a particular state and reject others. The (A), (B), and (C) filters select a', b', and c', respectively. We want to calculate the probability of getting $|c'\rangle$ when the beam is normalized to unity after the first filter (A). We find the probability as in the following:

$$(1.45) \qquad P(c'|b')P(b'|a') = \left|\left\langle c'\middle|b'\right\rangle\right|^2\left|\left\langle b'\middle|a'\right\rangle\right|^2.$$

The sum over b' to consider all b' paths is taken,

$$(1.46) \qquad \sum_{b'} P(c'|b')P(b'|a').$$

Let us look at an example with a different arrangement, and in this arrangement the (B) filter does not operate. Then the probability of obtaining $|c'\rangle$ is just $|\langle c'|a'\rangle|^2$,

which we can write as follows:

$$(1.47) \quad \left|\left\langle c'\middle|a'\right\rangle\right|^2 = \left|\sum_{b'}\left\langle c'\middle|b'\right\rangle\left\langle b'\middle|a'\right\rangle\right|^2$$

$$= \sum_{b'}\sum_{b''}\left\langle c'\middle|b'\right\rangle\left\langle b'\middle|a'\right\rangle\left\langle a'\middle|b''\right\rangle\left\langle b''\middle|c'\right\rangle$$

The state $\left|a'\right\rangle$ can be written in terms of the B eigenkets

$$(1.48) \quad \left|a'\right\rangle = \sum_{b'}\left|b'\right\rangle\left\langle b'\middle|a'\right\rangle,$$

We sum over the values of b', which correspond to all possible paths. The probability of obtaining c' depends on whether or not we perform (B) measurements.

1.7 The Uncertainty Relation

We will discuss the uncertainty relation in this section. For an observable A, the following operator is given:

$$(1.49) \quad \Delta A = A - \langle A\rangle.$$

The average value of $(\Delta A)^2$ (the dispersion of A) is

$$(1.50) \quad \langle(\Delta A)^2\rangle = \langle A^2 - 2A\langle A\rangle + \langle A\rangle^2\rangle$$

$$= \langle A^2\rangle - \langle A\rangle^2$$

The last line of 1.50 is an alternative way of expressing dispersion, which is also called *mean square deviation*, or *variance*. If the average is taken for an eigenstate of A, dispersion is equal to zero. For example, for the S_z+ state, the variance of S_x is found as below:

$$(1.51) \quad \langle S_x{}^2\rangle - \langle S_x\rangle^2 = \frac{\hbar^2}{4}.$$

We now explain the uncertainty relation. We have two observables, A and B. The following inequality is valid for any state:

$$(1.52) \quad \langle(\Delta A)^2\rangle\langle(\Delta B)^2\rangle \geq \frac{1}{4}|\langle[A,B]\rangle|^2.$$

For proof, we need to state three theorems.

Theorem 1.2 *The Schwarz inequality is given in the following:*

$$\langle \alpha | \alpha \rangle \langle \beta | \beta \rangle \geq |\langle \alpha | \beta \rangle|^2, \tag{1.53}$$

which is similar to

$$|\boldsymbol{a}|^2 |\boldsymbol{b}|^2 \geq |\boldsymbol{a} \cdot \boldsymbol{b}|^2 \tag{1.54}$$

in real space.

Theorem 1.3 *We obtain a real number when the average value of a Hermitian operator is taken.*

Theorem 1.4 *When we calculate the average value of an anti-Hermitian operator, shown as*

$$C = -C^\dagger, \tag{1.55}$$

we get an imaginary number.

Using these theorems, we can prove the uncertainty relation given in 1.52. We make use of Theorem 1.2 with

$$|\alpha\rangle = \Delta A \,|\rangle, \tag{1.56}$$

$$|\beta\rangle = \Delta B \,|\rangle. \tag{1.57}$$

Then we obtain the following inequality:

$$\langle (\Delta A)^2 \rangle \langle (\Delta B)^2 \rangle \geq |\langle \Delta A \Delta B \rangle|^2 \tag{1.58}$$

Blank kets are used because they may be any state. Note that A and B are Hermitian operators. We evaluate the right-hand side of Equation 1.58, but first, we write

$$\Delta A \Delta B = \frac{1}{2}[A, B] + \frac{1}{2}\{A, B\}. \tag{1.59}$$

$[\Delta A, \Delta B] = [A, B]$, and

$$([A, B])^\dagger = (AB - BA)^\dagger = BA - AB = -[A, B], \tag{1.60}$$

which means that $[A, B]$ is an anti-Hermitian operator. In contrast,

$$(1.61) \qquad \{A, B\}^\dagger = \{A, B\}.$$

So, on the right-hand side of the following equation,

$$(1.62) \qquad \langle \Delta A \Delta B \rangle = \frac{1}{2} \langle [A, B] \rangle + \frac{1}{2} \langle \{A, B\} \rangle,$$

the first term is purely imaginary, whereas the second is purely real. We have used Theorems 1.3 and 1.4. Then,

$$(1.63) \qquad |\langle \Delta A \Delta B \rangle|^2 = \frac{1}{4} |\langle [A, B] \rangle|^2 + \frac{1}{4} |\langle \{A, B\} \rangle|^2.$$

From Equation 1.58, we know that

$$(1.64) \qquad \langle (\Delta A)^2 \rangle \langle (\Delta B)^2 \rangle \geq \frac{1}{4} |\langle [A, B] \rangle|^2 + \frac{1}{4} |\langle \{A, B\} \rangle|^2.$$

The proof of the uncertainty relation is complete.

In the next section, we will discuss quantum contextuality in detail; but I want to briefly mention its possible relation with the uncertainty relation. Since spin measurement operators are used to test classical inequalities, possible uncertainty relations may be investigated regarding the spin measurements used in various contextuality scenarios. This is an open problem of whether one may determine the degree of contextuality using uncertainty relations. These uncertainties likely determine the degree of contextuality.

2. QUANTUM CONTEXTUALITY AND ENTANGLEMENT

We are familiar with classical physics in our daily lives because it is usually observable with the naked eye. It is easier to make a connection between what is happening and its numeric calculations. This is, however, not the case for quantum physics. Some of the main reasons are: 1) Unlike in macro scale measurements, some observables cannot be measured simultaneously beyond an uncertainty limit (The Heisenberg uncertainty) (Heisenberg, 1927); 2) Quantum Physics is about what happens in microscopic scales, so naked eyes are not helpful for observation; 3) Observer affects the outcome when s/he observes; 4) Deterministic approach of classical physics is not valid for quantum phenomena; in other words, the probabilistic approach is what one may use to determine possible outcomes of a measurement. The fourth item will be mainly discussed in this thesis. It has been discussed if Quantum Theory is a complete one (Einstein et al., 1935). In this context, it has been widely discussed, and a new approach has been proposed that there may be a hidden variable that may be why we need the probability theory. Along this direction, in the following section, we will discuss the Einstein-Podolsky–Rosen (EPR) experiment (Einstein et al., 1935) and the Bell inequality (Bell, 1966), which are the milestones of ongoing discussions during the 20th century.

2.1 EPR and the Bell Inequality

As mentioned earlier, an observer acts as a part of the observed in some sense. This is not the case for classical objects large enough to ignore small-scale corrections imposed by Quantum Theory (QT). For example, when we see someone riding a bicycle, we see ourselves independent of the moving objects, a human and a bicycle in this case. This is not true while observing subatomic particles; an observer is part of the physical system. According to QT, a particle does reveal physical properties

as a part of the act of observation. Otherwise, as long as physical property is not measured, that particle is not in a revealed state.

This initiated discussions among physicists, some of whom did not agree with the probabilistic interpretation of QT. Albert Einstein was one of the famous scientists who rejected the idea. In the famous EPR paper, he and co-authors Rosen and Podolsky proposed a thought experiment, claiming that quantum mechanics is not complete as a theory (Einstein et al., 1935). Let us check the following example to understand what Einstein means by "spooky action": Suppose we have a maximally entangled two-qubit state

$$|\psi\rangle = \frac{|01\rangle - |10\rangle}{\sqrt{2}}. \tag{2.1}$$

We have two agents, Alice and Bob, performing measurements on their respective qubits. When Alice measures one of the qubits, she can predict the outcome of Bob's measurement with certainty. Alice acquires the information on the outcome of Bob's measurement instantaneously, which is incompatible with the fact that transmitting information cannot be faster than the speed of light.

Nearly thirty years after the EPR paper was published, Bell's experiment showed that QT is compatible with Nature, and invalidated the EPR paper (Bell, 1966). The result Bell found gave us the famous Bell's inequality, which specifies the classical range to be violated by quantum mechanics. The Clauser-Horne-Shimony-Holt CHSH inequality is an example of Bell inequalities (Clauser et al., 1969). In this measurement scenario, there are two agents again, Alice and Bob, and we have a quantum system of two qubits. Observers are far away from each other and measure spins of their respective qubits. Alice performs measurements on the first qubit, whereas Bob measures the second one. Alice wants to measure the following observables: $A_1 = Z$, $A_2 = X$ where Z and X are the usual Pauli spin matrices. Bob wants to measure the following observables:

$$B_1 = -(Z + X)/\sqrt{2} \tag{2.2}$$

and

$$B_2 = (Z - X)/\sqrt{2}. \tag{2.3}$$

Bell defines the following the quantity

$$\mathbb{S}_{Bell} = A_1 B_1 + A_1 B_2 + A_2 B_1 - A_2 B_2 \tag{2.4}$$

which can be redefined as follows:

$$(2.5) \qquad \mathbb{S}_{Bell} = (A_1 + A_2)B_1 + (A_1 - A_2)B_2.$$

Alice and Bob get two values for each measurement, $+1$ and -1. When $A_1 = A_2$,

$$(2.6) \qquad \mathbb{S}_{Bell} = 2A_{1,2}B_1.$$

It is easy to see that $\mathbb{S}_{Bell} = \pm 2$. When $A_1 \neq A_2$,

$$(2.7) \qquad \mathbb{S}_{Bell} = 2A_1 B_1, \quad or \quad -2A_2 B_1.$$

In any case, $\mathbb{S}_{Bell} = \pm 2$. We already defined the observables A_i and B_i with Pauli matrices so that we can write the following

$$(2.8) \qquad \mathbb{S}_{Bell} = Z \otimes \frac{-(Z+X)}{\sqrt{2}} + Z \otimes \frac{Z-X}{\sqrt{2}} + X \otimes \frac{-(Z+X)}{\sqrt{2}} + X \otimes \frac{Z-X}{\sqrt{2}}.$$

The average of this Bell operator for a state

$$|\psi\rangle = \frac{|01\rangle - |10\rangle}{\sqrt{2}}$$

is given by

$$(2.9) \qquad \langle S_{Bell} \rangle = 2\sqrt{2}.$$

This exceeds the classical upper bound shown in the Bell inequality. The violation of the Bell inequality tells us that the classical predictions are not accurate in Nature. On the contrary, QT is well obeyed by Nature. Recall that it does not matter how far Alice and Bob are from each other. Distance between them does not affect the outcome. The assumption that Alice does not influence the result of Bob's measurement is called 'locality' which is invalid since one's measurement determines the other. In conclusion, our common sense about how the world works is wrong, and we must deepen our understanding of physics to develop a good intuition.

2.2 Quantum Non-Locality

As mentioned in the previous section, the principle of locality says that one's action on a physical state does not affect another physical state instantaneously; in other words, physical actions are locally bounded according to this principle. However, as seen before, local boundaries imposed by the Bell inequality are exceeded by measurements. Breaking the locality rule implies a new principle called 'quantum non-locality'. This is a counterintuitive principle incompatible with our daily life experience because we observe physical actions and define them locally. Local limitations in classical physics govern any effect of physical activity.

Some physicists were reluctant to accept the probabilistic interpretations of quantum mechanics, and some have argued that the outcomes of measurements appear probabilistic due to unknown parameters. Until 1964, it may have been thought that the theories based on hidden variables would give no different predictions. Then we would have two approaches giving the same results while one tells there are unknown parameters. Do we need such unknown parameters while we have a theory giving the same results without any hidden variable? During these discussions, J. S. Bell found an inequality to test the hidden variable model; however, it gave results compatible with quantum mechanical predictions (Bell, 1966). This is the Bell inequality mentioned in the previous section. We think that the most important result of the violation of Bell's inequality is that we do not consider position, x. Position is irrelevant in such a way that many physicists were irritated. Position in no way can affect the outcome of measurements, which shows us that there is no locality (non-locality). This is a unique feature of QT. The hidden variable model has been discussed widely; however, it has been ruled out by many works (Bell, 1966; Specker, 1960; Kochen & Specker, 1967; Bell, 1964; Aspect et al., 1982; Freedman & Clauser, 1972). For further reading, please refer to (Sakurai & Napolitano, 2011) and (Budroni et al., 2022).

2.3 Quantum Contextuality

In the rest of this chapter, we will focus on another unique feature of QT: quantum contextuality. First, we will discuss the pioneering work by Kochen and Specker (KS) (Kochen & Specker, 1967) and some other scenarios in which quantum contextuality has been shown. Later on, we will mention the KCBS inequality which is the simplest example of KS-like scenarios (Klyachko, 2002; Klyachko et al., 2008). A qutrit-system, a three-level quantum system, was studied to find possible contextual properties in this scenario.

2.3.1 KS-like Scenarios

Kochen and Specker, who used 117 projective measurements in the real three-dimensional space (Kochen & Specker, 1967), have proven Quantum contextuality for the first time. Since then, many state-independent and state-dependent measurement scenarios have been proposed to simplify measurement systems by reducing the number of observables. State-independent means that one can observe quantum contextuality for any state in a specific class; however, one should look into the specific quantum states in a class to observe contextuality in state-dependent scenarios. So much has been achieved, and the number of measurements drastically decreased. In the following subsections, we will discuss the simplified versions of KS-like measurement scenarios that do not require a specific group of qutrits to exhibit contextuality.

2.3.1.1 State-Independent Proof of Quantum Contextuality with 13 Observables

Yu and Oh succeeded in revealing contextuality by using only 13 projective measurements (Yu & Oh, 2012). Consider the observable

(2.10) $$A_i = \mathbb{I} - 2 \left| v_i \right\rangle \left\langle v_i \right|$$

where $\mathbb{I}$ is the identity matrix. $|v_i\rangle$ are the state vectors defined by Yu and Oh. The set of these vectors is in the following:

$$\frac{1}{\sqrt{3}}\begin{pmatrix} -1 \\ 1 \\ 1 \end{pmatrix}, \quad \frac{1}{\sqrt{2}}\begin{pmatrix} 0 \\ 1 \\ \pm 1 \end{pmatrix}, \quad \begin{pmatrix} 1 \\ 0 \\ 0 \end{pmatrix}, \quad \frac{1}{\sqrt{3}}\begin{pmatrix} 1 \\ -1 \\ 1 \end{pmatrix}, \quad \frac{1}{\sqrt{2}}\begin{pmatrix} 1 \\ 0 \\ \pm 1 \end{pmatrix},$$

$$\begin{pmatrix} 0 \\ 1 \\ 0 \end{pmatrix}, \quad \frac{1}{\sqrt{3}}\begin{pmatrix} 1 \\ 1 \\ -1 \end{pmatrix}, \quad \frac{1}{\sqrt{2}}\begin{pmatrix} 1 \\ \pm 1 \\ 0 \end{pmatrix}, \quad \begin{pmatrix} 0 \\ 0 \\ 1 \end{pmatrix}, \quad \frac{1}{\sqrt{3}}\begin{pmatrix} 1 \\ 1 \\ 1 \end{pmatrix}.$$

We should note that there are three eigenstates for each A_i, two of which have the same eigenvalue $+1$, and one has the eigenvalue -1. This is a semi-degenerate system.

The following inequality must be satisfied for a non-contextual system to be valid,

$$(2.11) \quad \kappa = \frac{1}{2}\left(\sum_{i=1}^{4}\langle A_i\rangle - \sum_{i=1}^{4}\sum_{j=5}^{10}\Gamma_{ij}\langle A_i A_j\rangle \right) + \sum_{k=5}^{13}\langle A_k\rangle - \sum_{m=5}^{12}\sum_{n>m}^{13}\Gamma_{mn}\langle A_m A_n\rangle \leqslant 9.$$

The authors set the following condition:

$$\Gamma_{ij} = 1 \quad \text{for} \quad \langle v_i | v_j\rangle = 0,$$
$$\Gamma_{ij} = 0 \quad \text{for} \quad \langle v_i | v_j\rangle \neq 0.$$

If one checks all possible assignments of values, $+1$ and -1, s/he can see that the upper bound can not be exceeded. This is very similar to the Bell case where we assign the same values to measurement outcomes; however, there is also a lower bound in addition to an upper bound. When we perform measurements on qutrit states, Equation 2.11 gives the following:

$$(2.12) \qquad\qquad\qquad \kappa = \frac{29}{3} = 9 + \frac{2}{3}.$$

To note, Equation 2.11 is the improved version of Yu and Oh's proposal (Cabello et al., 2012) to make it experimentally more easily testable. The inequality given in Equation 2.11 is violated by any qutrit state; therefore, it is a state-independent contextuality.

Cabello et al. (Cabello et al., 2012) transformed this non-contextual inequality into a Bell inequality, saying that performing two compatible measurements on a single qutrit is the same as performing them on two separated qutrit states which are

entangled as follows:

$$(2.13) \qquad |\psi\rangle = \frac{1}{\sqrt{3}} \Big(|0\rangle_1 |0\rangle_2 + |1\rangle_1 |1\rangle_2 + |2\rangle_1 |2\rangle_2 \Big).$$

Since there are observers, Alice and Bob, one needs to determine how to distribute these measurements between them. Alice is responsible for the measurements A_i ($i = 1, \ldots, 4,11,12,13$) while Bob performs measurements $B_j \equiv A_j$ ($j = 5, \ldots, 10$). Then the inequality in Equation 2.11 is transformed into a Bell-type non-contextual inequality

$$
\begin{aligned}
(2.14) \qquad \kappa' = \tfrac{1}{2} & \Big(\textstyle\sum_{i=1}^{4}\langle A_i\rangle - \sum_{i=1}^{4}\sum_{j=5}^{10}\Gamma_{ij}\langle A_i B_j\rangle \Big) + \sum_{j=5}^{10}\langle B_j\rangle + \sum_{k=11}^{13}\langle A_k\rangle \\
& - \textstyle\sum_{k=11}^{13}\sum_{j=5}^{10}\Gamma_{kj}\langle A_k B_j\rangle - \langle A_{11}A_{12}\rangle - \langle A_{11}A_{13}\rangle - \langle A_{12}A_{13}\rangle - \langle B_5 B_6\rangle \\
& - \langle B_7 B_8\rangle - \langle B_9 B_{10}\rangle \leqslant 9.
\end{aligned}
$$

For the state given in Equation 2.13,

$$\langle A_i B_i\rangle = 1 \quad \text{for} \quad i = 1, ..., 13.$$

By using this, Cabello et al. were able to replace $\langle A_i A_j\rangle$ and $\langle B_i B_j\rangle$ with

$$(2.15) \qquad \frac{1}{2}\Big(\langle A_i B_j\rangle + \langle A_j B_i\rangle - \langle A_i B_i\rangle - \langle A_j B_j\rangle \Big).$$

One then can obtain the following inequality,
(2.16)
$$
\begin{aligned}
\beta = \tfrac{1}{2} & \Big(\textstyle\sum_{i=1}^{4}\langle A_i\rangle - \sum_{i=1}^{4}\sum_{j=5}^{10}\Gamma_{ij}\langle A_i B_j\rangle + \sum_{j=5}^{10}\langle A_j B_j\rangle - \sum_{j=5}^{10}\sum_{m=5}^{10}\Gamma_{jm}\langle A_j B_m\rangle \\
& - \textstyle\sum_{k=11}^{13}\sum_{n=11}^{13}\Gamma_{kn}\langle A_k B_n\rangle \Big) + \sum_{j=5}^{10}\langle B_j\rangle + \sum_{k=11}^{13}\langle A_k\rangle - \sum_{k=11}^{13}\sum_{j=5}^{10}\Gamma_{kj}\langle A_k B_j\rangle \\
& + \textstyle\sum_{k=11}^{13}\langle A_k B_k\rangle \leqslant 15.
\end{aligned}
$$

When the given two-qutrit state is measured, it gives

$$(2.17) \qquad \langle\beta\rangle = \frac{47}{3} = 15 + \frac{2}{3}.$$

Again we see a violation, which means that Cabello et al. successfully derived a non-contextual inequality violated by any two-qutrit state (Cabello et al., 2012). Equation 2.16 is in the form of a Bell-type inequality. Its importance comes from the fact that it provides a link between the contextuality of a single qutrit and the non-locality of an entangled pair. The observables are the same, with the difference in how the measurements are performed. Yu and Oh perform measurements sequentially on the same system, whereas Cabello et al. do this on different systems.

2.3.1.2 Contextuality of Qutrit States in a Nine-observable System

Reducing the number of measurements has been of great importance in understanding contextuality in QT and can be essential in quantum information processing as well. Simplification of measurement systems sheds light on how fundamental feature contextuality is. Along this direction, it has been shown that one can find nine observables to observe contextuality for qutrits (Kurzyński & Kaszlikowski, 2012). The authors used the following rays:

$$|1\rangle = \begin{pmatrix} 1 \\ 0 \\ 0 \end{pmatrix}, \quad |2\rangle = \begin{pmatrix} 0 \\ 1 \\ 0 \end{pmatrix}, \quad |3\rangle = \begin{pmatrix} 0 \\ 0 \\ 1 \end{pmatrix}, \quad |4\rangle = \frac{1}{\sqrt{2}} \begin{pmatrix} 0 \\ 1 \\ -1 \end{pmatrix}, \quad |5\rangle = \frac{1}{\sqrt{3}} \begin{pmatrix} 1 \\ 0 \\ -\sqrt{2} \end{pmatrix},$$

$$|6\rangle = \frac{1}{\sqrt{3}} \begin{pmatrix} 1 \\ \sqrt{2} \\ 0 \end{pmatrix}, \quad |7\rangle = \frac{1}{2} \begin{pmatrix} \sqrt{2} \\ 1 \\ 1 \end{pmatrix}, \quad |8\rangle = \frac{1}{2} \begin{pmatrix} \sqrt{2} \\ -1 \\ -1 \end{pmatrix}, \quad |9\rangle = \frac{1}{2} \begin{pmatrix} \sqrt{2} \\ -1 \\ 1 \end{pmatrix}.$$

One assigns either 1 or 0 to observables, distributing them in any possible scenario. As a result, one obtains the expectation values in the classical range for all possible cases. Using the argument in (Kurzyński & Kaszlikowski, 2012), it was shown that the classical upper bound is given by

$$(2.18) \qquad\qquad \sum_{i=1}^{9} \langle \Pi_i \rangle \leqslant 3$$

where $\Pi_i = |i\rangle \langle i|$. One can define the following observable,

$$(2.19) \qquad\qquad A_i = 1 - 2\Pi_i.$$

Then,

$$(2.20) \qquad A_i A_j = (1 - 2\Pi_i)(1 - 2\Pi_j) = 1 - 2\Pi_j - 2\Pi_i + 4\Pi_i \Pi_j$$

which gives

$$(2.21) \qquad\qquad A_i A_j = 1 - 2\Pi_j - 2\Pi_i$$

when $|i\rangle$ and $|j\rangle$ are orthogonal to each other. Using this relation, one obtains the following inequality,

$$(2.22) \qquad \sum_{(i,j)\in E(G)} \langle A_i A_j \rangle + \langle A_9 \rangle \geq -4$$

where $E(G)$ denotes the set of neighboring edges in the graph G. G is explicitly illustrated in (Kurzyński & Kaszlikowski, 2012), showing the orthogonality relations among nine rays. Equation 2.18 can be expressed as follows:

$$(2.23) \qquad \sum_{i=1}^{9} \langle \Pi_i \rangle = \langle C \rangle.$$

C is equivalent to the summation of all projective measurements. Its eigenvalues are

$$(2.24) \qquad \lambda_1 = \frac{10}{3}, \quad \lambda_2 = 3, \quad \lambda_3 = \frac{8}{3}.$$

The authors used the argument that any density matrix, whose eigenvectors are $|\psi_1\rangle$, $|\psi_2\rangle$, and $|\psi_3\rangle$, can be in a diagonal form,

$$(2.25) \qquad \rho = p |\psi_1\rangle \langle \psi_1| + q |\psi_2\rangle \langle \psi_2| + r |\psi_3\rangle \langle \psi_3|,$$

provided that

$$(2.26) \qquad p \geqslant q \geqslant r.$$

One can calculate the expectation value of C as follows:

$$(2.27) \qquad \langle C \rangle = Tr(\rho C) = \frac{1}{3}(10p + 9q + 8r)$$

which gives

$$(2.28) \qquad \langle C \rangle = 3 + \frac{p-r}{3}$$

due to the normalization condition,

$$(2.29) \qquad q = 1 - p - r.$$

$\langle C \rangle = 3$ when $p = r = 1/3$; otherwise, one obtains a result above the classical upper bound, which means the inequality in Equation 2.18 is violated. This is very similar to the CHSH scenario (Clauser et al., 1969) because one has to properly arrange rays on which measurements are performed to observe contextuality. This
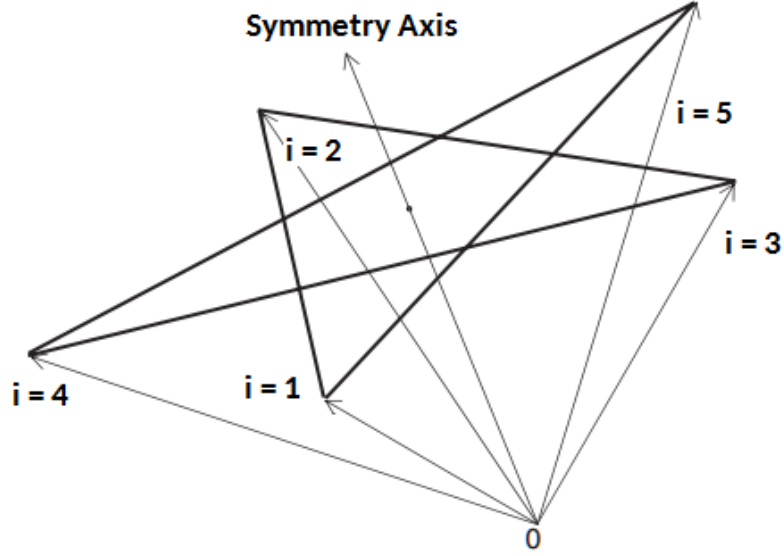
Figure 2.1 We have unit vectors whose ends correspond to five corners of the penta-gram. One performs each measurement along a unit vector. We have the following condition for the vectors: $i \perp i+1$. We also show the symmetry axis of the penta-gram. We have adapted this figure from the original KCBS article (Klyachko et al., 2008)

work concludes that one can find nine projective measurements for any qutrit state to observe quantum contextuality. We emphasize that nine projectors should be determined separately for each qutrit.

2.3.2 The KCBS Scenario

In this section, we will talk about the KCBS scenario, including five projective measurements performed on a three-level quantum system (Klyachko et al., 2008). The setting is based on a spin-1 system to demonstrate the contextuality of a qutrit system. The following observables are defined,

$$(2.30) \qquad\qquad A_i = 2S_i^2 - 1$$

where S_i are spin projection measurements, and $i = 1, 2, ..., 5$. We know that, for a spin-1 system, there are three non-degenerate eigenstates with eigenvalues -1, 0, and 1. For spin values +1 and -1, one can see that we get the same eigenvalue when A_i is measured. We may argue that the system is made into a semi-degenerate three-level quantum system. We now have two eigenvalues, +1 and -1. A_i and A_j commute

24

when $\hat{n}_i \perp \hat{n}_j$. Authors discovered five directions along which one can measure both A_i and A_{i+1}. The following inequality must be satisfied for any non-contextual system,

$$(2.31) \qquad \langle A_1 A_2 \rangle + \langle A_2 A_3 \rangle + \langle A_3 A_4 \rangle + \langle A_4 A_5 \rangle + \langle A_5 A_1 \rangle \geq -3.$$

The KCBS operator, which corresponds to

$$(2.32) \qquad \sum_{i \bmod 5} A_i A_{i+1},$$

is a diagonal matrix given as:

$$(2.33) \qquad S_{KCBS} = \begin{pmatrix} -5+2\sqrt{5} & 0 & 0 \\ 0 & 5-4\sqrt{5} & 0 \\ 0 & 0 & -5+2\sqrt{5} \end{pmatrix}.$$

It was shown that for the neutrally polarized spin state (with spin value 0) given as

$$(2.34) \qquad |0\rangle = \begin{pmatrix} 0 \\ 1 \\ 0 \end{pmatrix},$$

we get

$$(2.35) \qquad \langle 0| S_{KCBS} |0\rangle = \begin{pmatrix} 0 \\ 1 \\ 0 \end{pmatrix}^T \cdot \begin{pmatrix} -5+2\sqrt{5} & 0 & 0 \\ 0 & 5-4\sqrt{5} & 0 \\ 0 & 0 & -5+2\sqrt{5} \end{pmatrix} \cdot \begin{pmatrix} 0 \\ 1 \\ 0 \end{pmatrix}$$
$$= 5-4\sqrt{5} \;\; (\simeq -3.94)$$

This is the lower quantum limit exceeding the classical bound; in other words, this is the lowest value. That is a remarkable result because it tells us quantum systems are intrinsically contextual, and there is no need for entanglement to observe non-classical behaviors. For the eigenket $|1\rangle$, we obtain the following result:

$$(2.36) \qquad \langle 1| S_{KCBS} |1\rangle = \begin{pmatrix} 1 \\ 0 \\ 0 \end{pmatrix}^T \cdot \begin{pmatrix} -5+2\sqrt{5} & 0 & 0 \\ 0 & 5-4\sqrt{5} & 0 \\ 0 & 0 & -5+2\sqrt{5} \end{pmatrix} \cdot \begin{pmatrix} 1 \\ 0 \\ 0 \end{pmatrix}$$
$$= -5+2\sqrt{5} \;\; (\simeq -0,53).$$

We get the same result for the eigenket $|-1\rangle$. As one can see, these results are within the classical range. Moreover, if we take the average of the KCBS operator for the homogeneous linear combination of the kets $|\pm 1\rangle$, we still obtain the same result ($\simeq -0,53$). However, in the following section, we will see that the maximal violation of the KCBS inequality is possible when one considers the homogeneous combination of these kets when rotated.

2.3.3 Contextual Retrit States in the KCBS Scenario

The outline of this subsection is as follows: In Section 2.3.3.1, we investigate the symmetry of the KCBS inequality through the rotational analysis (Diker & Gedik, Diker & Gedik). In sections 2.3.3.2, 2.3.3.3 and 2.3.3.4 we keep on this rotational analysis of the KCBS inequality for specific examples (Diker & Gedik, Diker & Gedik). In Section 2.3.3.5, we look into the real subgroup of qutrit states and classify them by their (non-)contextuality under certain rotations (Diker & Gedik, Diker & Gedik). In Section 2.3.3.6, we provide the data on Euler angles and the parameters of retrits. We also derive general formulas for them (Diker & Gedik, Diker & Gedik).

2.3.3.1 Rotational invariance of the KCBS-type contextuality

The KCBS inequality is the simplest example of non-contextual inequalities. The violation of this inequality shows us the contextual behavior of a particular group of qutrit systems. It includes only five measurements performed by one agent on a qutrit system. Within our knowledge, no one has not analyzed it, aiming at finding symmetries in the Euclidean space $\mathbb{E}^3$. For this purpose, we will first check if the KCBS operator is invariant under rotations about the symmetry axis (Z-axis). The operator for a rotation about Z-axis by an angle alpha:

$$(2.37) \qquad e^{-i\frac{S_z}{\hbar}\alpha}$$

which is equal to

$$(2.38) \qquad I - S_z{}^2(1 - \cos\alpha) - iS_z\sin\alpha.$$

We got this equation by expanding the exponential operator in power series. The matrix representation of the rotation operator is in the following:

$$(2.39) \qquad \begin{pmatrix} \cos(\alpha) - i\sin(\alpha) & 0 & 0 \\ 0 & 1 & 0 \\ 0 & 0 & \cos(\alpha) + i\sin(\alpha) \end{pmatrix}.$$

The KCBS operator is rotated around the Z-axis,

$$(2.40) \qquad e^{i\frac{S_z}{\hbar}\alpha} \left[A_1 A_2 + A_2 A_3 + A_3 A_4 + A_4 A_5 + A_5 A_1 \right] e^{-i\frac{S_z}{\hbar}\alpha}$$

which corresponds to the following matrix

$$\begin{pmatrix} -5 + 2\sqrt{5} & 0 & 0 \\ 0 & 5 - 4\sqrt{5} & 0 \\ 0 & 0 & -5 + 2\sqrt{5} \end{pmatrix}.$$

One can see the invariance of the KCBS operator under rotations around the Z-axis which is the symmetry axis of the pentagram; in other words, non-contextuality (or contextuality) is conserved for three-level quantum systems. This shows us that the pentagram illustrated in Figure 2.1 is a nontrivial diagram since it is also symmetric.

2.3.3.2 Contextuality Region for Spin-zero State

The neutrally polarized spin state denoted by $|0\rangle$ maximally violates the KCBS inequality. It can be called the most non-classical state in the KCBS scenario; however, we need to ask whether one can observe contextuality for this state if rotated in the physical space. For this purpose, we analyze the KCBS operator denoted by S through rotations as follows:

$$(2.41) \qquad e^{i\frac{S_z}{\hbar}\alpha} e^{i\frac{S_y}{\hbar}\beta} e^{i\frac{S_z}{\hbar}\gamma} S e^{-i\frac{S_z}{\hbar}\gamma} e^{-i\frac{S_y}{\hbar}\beta} e^{-i\frac{S_z}{\hbar}\alpha} = S'.$$

Note that α, β and γ are Euler angles. The expectation value for the $|0\rangle$ state is

$$(2.42) \qquad \langle 0| S' |0\rangle = (5 - 3\sqrt{5})\cos 2\beta - \sqrt{5}$$

which is a function of β, i.e., the only rotations we need to consider are the ones around the Y-axis. The set of β values satisfying the following condition,

$$(2.43) \qquad \qquad \langle S' \rangle < -3$$

gives us the Euler angles for contextuality. The inequality in Equation 2.43 is satisfied for the following sets: $-31.717° < \beta < 31.717°$ and $148.283° < \beta < 211.717°$. This tells us that the maximally contextual state, the neutrally polarized spin state in our case, may behave classically under some rotations.

2.3.3.3 Non-contextuality of Spin-1 States is Invariant

In this section, we will check all rotations of the KCBS operator in the physical Euclidean space $\mathbb{E}^3$ to determine any group of five measurements for which the eigenstates of the spin-1 operator exhibits contextual behavior.

The neutrally polarized spin state is a maximally contextual quantum state violating the KCBS inequality under certain rotations. We will check if the other two eigenstates exhibit the same type of behavior. The general rotation operator is

$$(2.44) \qquad \qquad e^{-i\frac{S_z}{\hbar}\gamma} e^{-i\frac{S_y}{\hbar}\beta} e^{-i\frac{S_z}{\hbar}\alpha},$$

and the matrix form is as follows:

$$(2.45) \qquad D(\alpha,\beta,\gamma) = \begin{pmatrix} e^{-i\alpha-i\gamma}\cos^2\left(\frac{\beta}{2}\right) & -\frac{e^{-i\gamma}\sin(\beta)}{\sqrt{2}} & e^{i\alpha-i\gamma}\sin^2\left(\frac{\beta}{2}\right) \\ \frac{e^{-i\alpha}\sin(\beta)}{\sqrt{2}} & \cos(\beta) & -\frac{e^{i\alpha}\sin(\beta)}{\sqrt{2}} \\ e^{i\gamma-i\alpha}\sin^2\left(\frac{\beta}{2}\right) & \frac{e^{i\gamma}\sin(\beta)}{\sqrt{2}} & e^{i\alpha+i\gamma}\cos^2\left(\frac{\beta}{2}\right) \end{pmatrix}.$$

The KCBS operator, denoted by S, is rotated as follows:

$$(2.46) \qquad \qquad D^\dagger(\alpha,\beta,\gamma)SD(\alpha,\beta,\gamma) = S'(\alpha,\beta)$$

where S' depends on α and β. Z-axis is the symmetry axis of the KCBS pentagram, which is also rotated. The new symmetry axis is given as the following unit vector: $(\sin(\beta)\cos(\gamma), \sin(\beta)\sin(\gamma), \cos(\beta))$. The average of the new KCBS operator is found as

$$(2.47) \qquad \qquad \langle \pm 1 | S' | \pm 1 \rangle = \frac{1}{2}\left(\left(3\sqrt{5}-5\right)\cos(2\beta) + \sqrt{5} - 5\right),$$
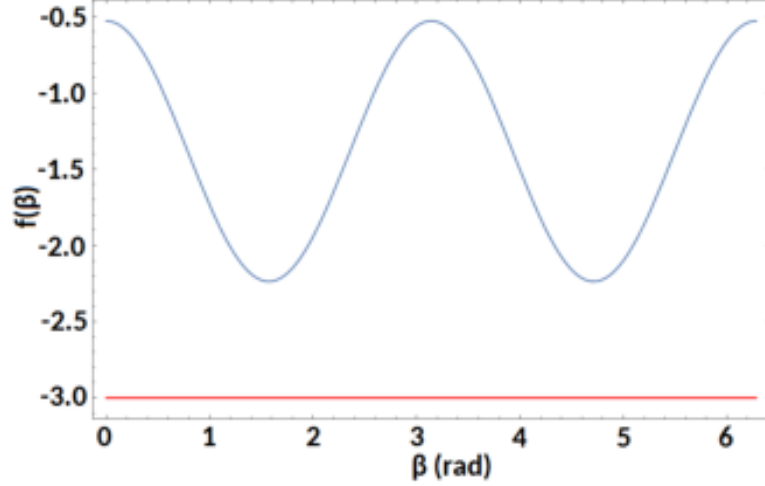
Figure 2.2 The average of the KCBS operator depends on α and repeats over intervals of π radians. The classical limit that is -3 is not violated. We observe that the spin states, having the spin values ± 1, exhibit non-contextuality not affected by rotations.

which means that the result depends on the rotation around the Y-axis. One may see the plot for this result in Figure 2.2.

2.3.3.4 Contextuality of Homogeneous Linear Combination of Spin-1

　　　　States

As mentioned earlier, the spin states, $|1\rangle$ and $|-1\rangle$ give us non-contextual results which are independent of rotations; in other words, we can not find any group of five measurements to observe contextuality in the KCBS scenario. Our next step is to check whether the homogeneous linear combination of those can violate the non-contextuality inequality. For this, we calculate the expectation value of $S'(\alpha, \beta)$,

$$ (2.48) \qquad \langle \psi | S'(\alpha, \beta) | \psi \rangle $$

where

$$ (2.49) \qquad |\psi\rangle = \frac{1}{\sqrt{2}}(|1\rangle + |-1\rangle). $$

We obtain

$$ (2.50) \quad \langle \psi | S'(\alpha, \beta) | \psi \rangle = \left(-5 + 2\sqrt{5}\right)\cos^2(\alpha) + \left(\left(-5 + 3\sqrt{5}\right)\cos(2\beta) - \sqrt{5}\right)\sin^2(\alpha), $$

29
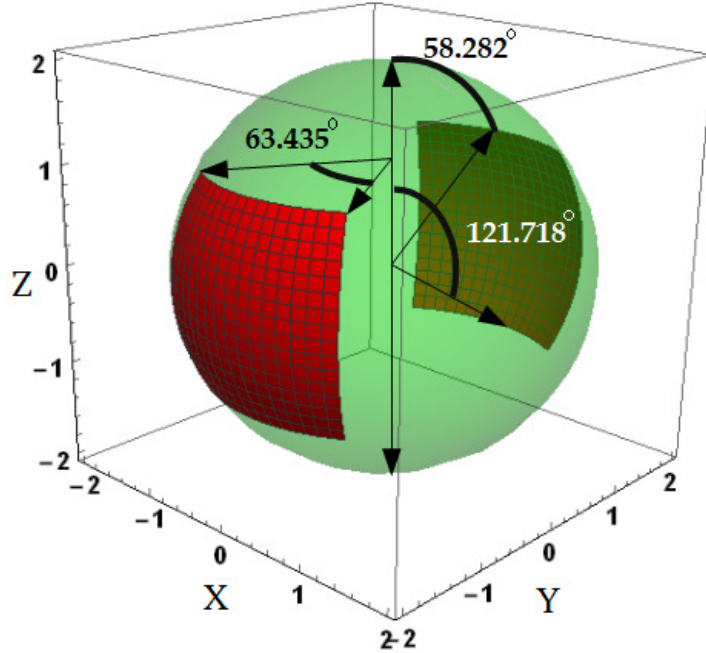
Figure 2.3 The rotation of the KCBS operator. Red surfaces on the sphere correspond to the contextual states for the homogeneous linear combination of $|1\rangle$ and $|-1\rangle$. We observe the spherical symmetry for the red surfaces. We specify the ranges of the Euler angles in degree units, for which we observe quantum contextuality.

which gives non-classical results for the following sets of Euler angles: $58.282° \leq \beta \leq 121.718°$ and $58.282° \leq \alpha \leq 121.718°$, or $238.283° \leq \alpha \leq 301.718°$. In Figure 2.3, the Euler angles, for which the KCBS inequality is violated, can be seen on the sphere. We have found two minima of this function for $\beta, \alpha = 90°$ and $\alpha = 270°$, $\beta = 90°$. We find $5 - 4\sqrt{5}$ for both minima, and the quantum state is maximally contextual. The average of the spin-1 operator for $|\psi\rangle$ is zero, as in the case of a zero-spin state, and both $|\psi\rangle$ and $|0\rangle$ are maximally contextual. Recall that $|1\rangle$ and $|-1\rangle$ do not exhibit contextuality when one measures separately in the KCBS scenario.

2.3.3.5 Classification of Retrit States

We work on the real subgroup of qutrit states and check if they are contextual under some rotations. We consider the real subgroup spanning all possible linear

combinations of $|0\rangle$, $|1\rangle$, and $|-1\rangle$. The general form of a retrit state is as follows:

$$(2.51) \qquad |\psi\rangle = a\,|1\rangle + b\,|0\rangle + c\,|-1\rangle$$

where $a, b, c \in \mathbb{R}$. We may parameterize a retrit state by using spherical coordinates;

$$(2.52) \qquad \begin{aligned} |\psi\rangle &= \sin\theta\cos\phi\,|1\rangle + \sin\theta\sin\phi\,|0\rangle + \cos\theta\,|-1\rangle \\ &(0 \le \theta < \pi, \;\; 0 \le \phi < 2\pi). \end{aligned}$$

We rotate the KCBS operator and calculate the expectation value,

$$(2.53) \qquad \langle\psi|\,D^\dagger(\alpha,\beta,\gamma) S D(\alpha,\beta,\gamma)\,|\psi\rangle.$$

We obtain a function of α, β, θ and ϕ,

$$
\begin{aligned}
(2.54) \qquad f(\theta,\phi,\beta,\alpha) = \frac{1}{4}\Big(& 2((3\sqrt{5}-5)\cos(2\beta) + \sqrt{5}-5)\cos^2(\theta) \\
&+ (3\sqrt{5}-5)\sin^2(\theta)(\cos(2\beta)(3\cos(2\phi)-1) \\
&- 2\sqrt{2}\sin(2\beta)\cos(\alpha)\sin(2\phi)) \\
&+ 4(3\sqrt{5}-5)\sin(\beta)\sin(2\theta)(\sin(\beta)\cos(2\alpha)\cos(\phi) \\
&+ \sqrt{2}\cos(\beta)\cos(\alpha)\sin(\phi)) \\
&+ \sin^2(\theta)((3\sqrt{5}-5)\cos(2\phi) - \sqrt{5}-5)\Big).
\end{aligned}
$$

We could not find the analytic solution to this function of four variables because it is challenging; however, we may check the rotations of retrit states around the Y- and Z-axis with certain rotation angles. We may simplify Equation 2.54 by assigning values to β and α. This will help experimentalists to determine which Euler angles should be used.

In the first example, we check the case with no rotation ($\beta, \alpha = 0$), which gives

$$
\begin{aligned}
(2.55) \qquad f(\theta,\phi,0,0) = \frac{1}{4}\Big(& \sin^2(\theta)\left(\left(3\sqrt{5}-5\right)\cos(2\phi) - \sqrt{5}-5\right) \\
&+ \left(3\sqrt{5}-5\right)\sin^2(\theta)(3\cos(2\phi)-1) \\
&+ 2\left(4\sqrt{5}-10\right)\cos^2(\theta)\Big).
\end{aligned}
$$

By doing straightforward calculations, $f(\theta,\phi,\beta,\alpha)$ can be found for different Euler angles. The latter examples are for rotations around both Y- and Z-axis, or only

the Y-axis, which can be seen in the following:

$$f(\theta,\phi,\pi/2,0) = \frac{1}{4}\bigg(\sin^2(\theta)\left(\left(3\sqrt{5}-5\right)\cos(2\phi)-\sqrt{5}-5\right)$$
$$\text{(2.56)} \qquad\qquad + \left(3\sqrt{5}-5\right)\sin^2(\theta)(1-3\cos(2\phi))$$
$$+ 4\left(3\sqrt{5}-5\right)\sin(2\theta)\cos(\phi)-4\sqrt{5}\cos^2(\theta)\bigg),$$

$$f(\theta,\phi,\pi/4,0) = \frac{1}{8}\bigg(2\left(3\sqrt{5}-5\right)\sin^2(\theta)\left(\cos(2\phi)-2\sqrt{2}\sin(2\phi)\right)$$
$$\text{(2.57)} \qquad\qquad + 4\left(3\sqrt{5}-5\right)\sin(2\theta)\left(\sqrt{2}\sin(\phi)+\cos(\phi)\right)$$
$$+ \left(3\sqrt{5}-5\right)\cos(2\theta)+\sqrt{5}-15\bigg),$$

and

$$f(\theta,\phi,\pi/4,\pi/4) = \frac{1}{8}\bigg(4\left(3\sqrt{5}-5\right)\sin(2\theta)\sin(\phi)$$
$$\text{(2.58)} \qquad\qquad + 2\left(3\sqrt{5}-5\right)\sin^2(\theta)(\cos(2\phi)-2\sin(2\phi))$$
$$+ \left(3\sqrt{5}-5\right)\cos(2\theta)+\sqrt{5}-15\bigg).$$

In Figure 2.4, the region plots for Equations 2.55-2.58 are given. The red regions shown on the spheres shrink and rotate as we apply the general rotation operator to the KCBS operator. Whether we can observe contextuality in the KCBS scenario does not depend on rotations around the Z-axis. Rotations around Z-axis affect the result if and only if we rotate the KCBS operator around both Y-axis and Z-axis. This causes the red regions to expand or shrink depending on Euler angles. In conclusion, retrit states do not always exhibit contextual behavior in the KCBS scenario; in other words, a qutrit state may be intrinsically contextual, but it does not necessarily mean that we can observe quantum contextuality for any group of five measurements. Furthermore, for a set of Euler angles, any retrit state can not violate the KCBS inequality, i.e., they give results larger than the classical lower limit. Two examples of the set of Euler angles for which we do not find any contextual retrit state are provided: (1) $52.1° \le \beta \le 128°$, $232.2° \le \beta \le 308.1°$ where $\alpha = 41.8°$; (2) $32.9° \le \beta \le 61.5°$, $118.5° \le \beta \le 147.2°$, $213.0° \le \beta \le 241.6°$, and $298.7° \le \beta \le 327.3°$ where $\alpha = 104.5°$.
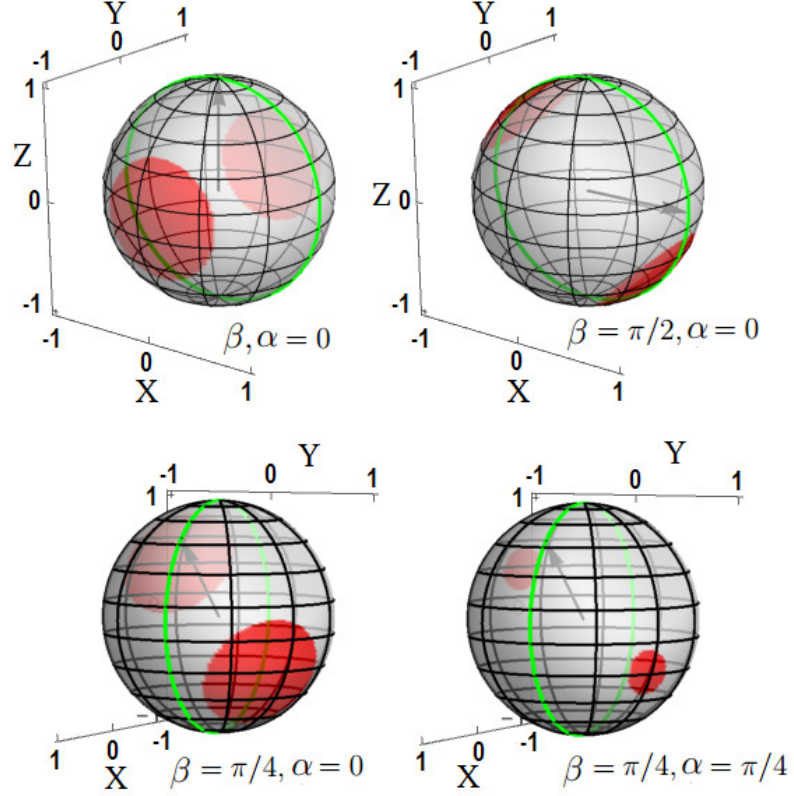
Figure 2.4 We give the set of contextual retrit states shown as red regions on four spheres under various rotations. The light grey region gives the set of non-contextual states. The thick black arrow shows the symmetry axis of the KCBS pentagram. The great circle is drawn to show the bows at $\phi = 0$ and $\phi = \pi$. The red regions shrink and rotate while the KCBS operator is being rotated.

2.3.3.6 Relations between Euler Angles and Spherically-parameterized

Retrit States

In this section, we will find correlations between Euler rotation angles and the degree of contextuality for retrit states by using the collected data. The general rotation operator is

$$e^{-i\frac{S_z}{\hbar}\gamma} e^{-i\frac{S_y}{\hbar}\beta} e^{-i\frac{S_z}{\hbar}\alpha},$$

where the last rotation around the Z-axis is ineffective, and we only take into account the first rotation around the Z-axis together with the rotation around the Y-axis. We need to determine the set of only β and α values for which we find maximally contextual retrits. Retrit states are shown in spherical coordinates as follows: $|\psi\rangle = (\sin\theta\cos\phi, \sin\theta\sin\phi, \cos\theta)$ where $0 \leq \phi < 2\pi$ and $0 \leq \theta < \pi$. There are four variables in total. We aim to find retrit states that violate the KCBS inequality maximally, and how they depend on Euler angles. Therefore, we need four relations where θ_{min} and ϕ_{min} represent values for the global minima of $f(\theta, \phi, \beta, \alpha)$. Global minima

33

are where we observe the maximal violation of the KCBS inequality. Finding the minima is essential; however, it is a hard problem even in the real subgroup of qutrits. Considering the most general solution, there are six parameters in total, making the solution even harder. Two extra parameters are added to the problem from phases. In our case, there are four variables in total. Instead of directly trying to solve the problem, we chose to collect data for minima where the following equation is satisfied:

$$(2.59) \qquad f(\theta_{min}, \phi_{min}, \beta_{min}, \alpha_{min}) = 5 - 4\sqrt{5},$$

which is the global minimum, i.e., the maximal contextuality. We acquired the data for θ_{min}, ϕ_{min}, β_{min} and α_{min}. One can see it in Table 2.1. This data is important for us to find possible trendlines between retrits and Euler angles and to show them on two-dimensional plots.

By assigning some values to β (rotation angle around Y-axis), we found α (rotation angle around Z-axis) values for which we observe maximal contextuality. We collected the data for each variable satisfying Equation 2.59. We assigned the following values to β:

$$\beta = 0, \frac{\pi}{16}, \frac{2\pi}{16}, \frac{3\pi}{16}, ..., \frac{15\pi}{16}, \pi$$

for each of which it is possible to find θ_{min}, ϕ_{min} and α_{min} values to obtain Equation 2.59. We found these values for each assigned value of β. We saw that $\alpha_{min} \in \{0, \pi\}$. This eases our job and narrows down the solution set. Through the graph analysis of Equation 2.59, we conjecture that β is continuously a part of the solution set for minima.

We now look for possible relations between β and ϕ (θ) values. We provided the data in Table 2.1 where one can see ϕ and θ values together with β values giving the global minima (α is taken to be 0). In Figure 2.5, one may see data points and its trendline on the β-ϕ graph given by:

$$(2.60) \qquad \phi_{min}(\beta) = 4.71239 - \beta.$$

Equation 2.60 gives us a straight line fitting almost perfectly; however, if one looks closely, the collected data points can be seen, following a curve fluctuating around the straight line. In light of this problem, we have added a trigonometric term with a small coefficient. As a result, we obtain a curve fitting better, and $\phi_{min}(\beta)$ can be rewritten in a corrected form:

$$(2.61) \qquad 4.71239 - \beta + (\frac{10}{59})\sin(2\beta).$$

Table 2.1

Euler Angle	Spherical Parameters of Retrits	
β_{min} (rad)	θ_{min} (rad)	ϕ_{min} (rad)
0	1.57080	4.71239
$\pi/16$	1.43240	4.57265
$2\pi/16$	1.29678	4.42746
$3\pi/16$	1.16707	4.27100
$4\pi/16$	1.04720	4.09691
$5\pi/16$	0.94229	3.89869
$6\pi/16$	0.85888	3.67149
$7\pi/16$	0.80443	3.41581
$8\pi/16$	0.78540	3.14159
$9\pi/16$	0.80443	2.86737
$10\pi/16$	0.85888	2.61169
$11\pi/16$	0.94229	2.38449
$12\pi/16$	1.04720	2.18628
$13\pi/16$	1.16707	2.01218
$14\pi/16$	1.29678	1.85572
$15\pi/16$	1.43240	1.71053
$16\pi/16$	1.57080	1.57080
$17\pi/16$	1.70919	1.43106
$18\pi/16$	1.84481	1.28587
$19\pi/16$	1.97452	1.12941
$20\pi/16$	2.09439	0.95532
$21\pi/16$	2.19930	0.75710
$22\pi/16$	2.28271	0.52990
$23\pi/16$	2.33716	0.27422
$24\pi/16$	2.35619	0
$25\pi/16$	2.33716	-0.27422
$26\pi/16$	2.28271	-0.52990
$27\pi/16$	2.19930	-0.75710
$28\pi/16$	2.09439	-0.95532
$29\pi/16$	1.97452	-1.12941
$30\pi/16$	1.84481	-1.28587
$31\pi/16$	1.70919	-1.43106
$32\pi/16$	1.57080	-1.57080
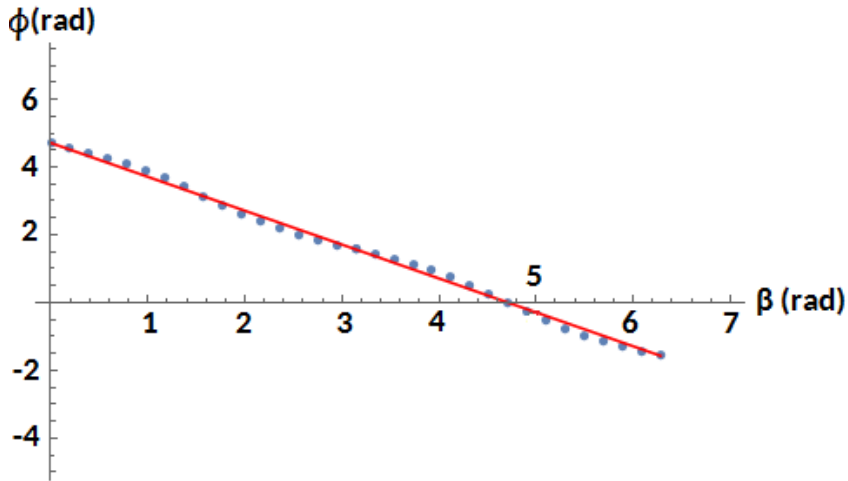
Figure 2.5 We show the data points taken for ϕ_{min} and its linear trendline with respect to β without correction.

The plot for Equation 2.61 is illustrated in Figure 2.6. In the next step, we will find how θ_{min} changes with rotation around the Y-axis. We can take α_{min} zero. One can see the collected points and the curve in Figure 2.7. From the figure, it can be seen that this is a usual trigonometric function with 2π-period. With some corrections, we may get the following:

$$(2.62) \qquad\qquad \theta_{min} = 1.57 - 0.77\sin(\beta).$$

The mathematical relations provided here are important because they provide the set of Euler angles for which one observes maximal quantum contextuality. The relations found are essential for experimental purposes. Recall that α_{min} can have two values, π or 0, for maximally-contextual states, making finding the whole solution set easier.
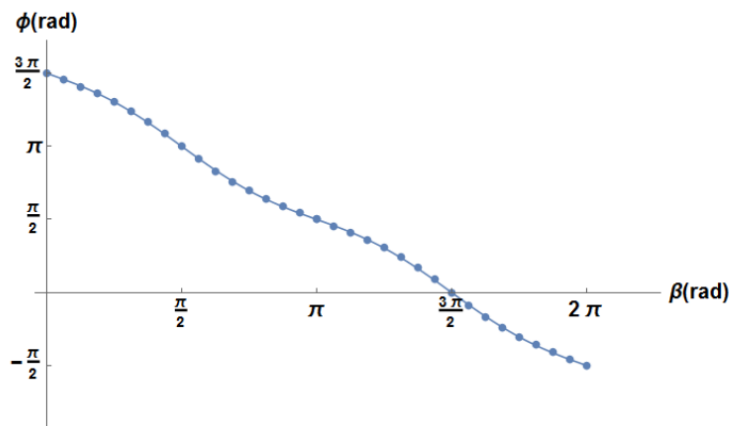
Figure 2.6 We show the data points taken for ϕ_{min} and its trendline with respect to β with correction. We obtain a better-fitting curve than the one in Figure 2.5.
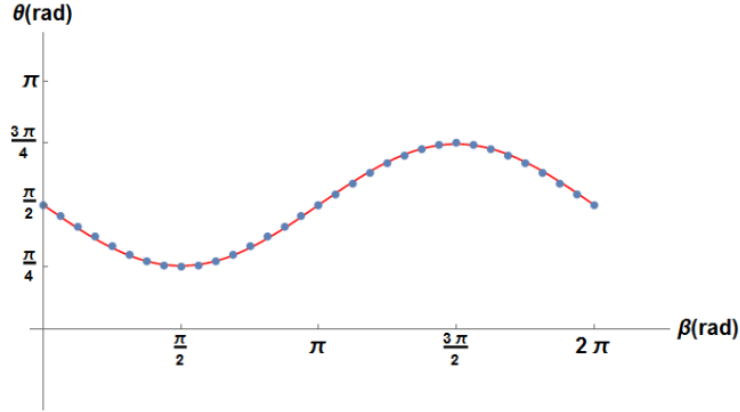
Figure 2.7 The plot of $\theta_{min}(\beta)$ which is a simple trigonometric function multiplied by a coefficient. We also add a constant.

We took α_{min} zero for our case. When $\alpha_{min} = \pi$, one should be able to find similar relations due to symmetry.

2.3.3.7 The Set of Contextual Qutrit States in the Real Hilbert Space

In this section, we look into the real subspace of Hilbert space to determine the always-non-contextual qutrit states; in other words, we will find the qutrit states that do not violate the KCBS inequality for arbitrary Euler angles in the physical space. We will check the subgroup spanning linear combinations of $|0\rangle$ and $|+\rangle$ where

$$(2.63) \qquad |+\rangle = \frac{1}{\sqrt{2}}(|1\rangle + |-1\rangle).$$

Basis states are the usual eigenstates of the spin-1 operator ($|0\rangle$, $|1\rangle$, and $|-1\rangle$ with spin values 0, 1, and -1). We use the qutrit state in the following form:

$$(2.64) \qquad |\psi\rangle = a|0\rangle + b|+\rangle$$

where $a, b \in \mathbb{R}$. We rotate the KCBS operator and then calculate the expectation value as follows:

$$(2.65) \qquad \langle\psi| D^\dagger(\theta, \alpha, \phi) S D(\theta, \alpha, \phi) |\psi\rangle$$

37

which has four variables in total, a, b, α and θ,

$$
\begin{aligned}
\Psi(a,b,\alpha,\theta) = {} & \sin^2(\alpha)\left(\left(2\sqrt{5}-5\right)a^2 - \left(4\sqrt{5}-5\right)b^2\sin^2(\theta)\right) \\
& + \cos^2(\alpha)\left(\left(5-4\sqrt{5}\right)a^2 + \left(2\sqrt{5}-5\right)b^2\sin^2(\theta)\right) \\
& + \left(2\sqrt{5}-5\right)b^2\cos^2(\theta).
\end{aligned}
$$

(2.66)

By using the normalization condition, one may reduce the number of variables. The equation can be rewritten as

$$
\begin{aligned}
\Psi'(a,\alpha,\theta) = {} & \sin^2(\alpha)\left(\left(4\sqrt{5}-5\right)\left(a^2-1\right)\sin^2(\theta) + \left(2\sqrt{5}-5\right)a^2\right) \\
& + \cos^2(\alpha)\left(\left(5-4\sqrt{5}\right)a^2 - \left(2\sqrt{5}-5\right)\left(a^2-1\right)\sin^2(\theta)\right) \\
& - \left(2\sqrt{5}-5\right)\left(a^2-1\right)\cos^2(\theta)
\end{aligned}
$$

(2.67)

where $b = \sqrt{1-a^2}$ or $-\sqrt{1-a^2}$. We need to find a values within the classical range; in other words, we aim to find a values for which any group of five measurements can not be found to observe the violation of KCBS inequality. We need to find the set of a values satisfying the following,

(2.68)
$$
\Psi'(a,\alpha,\theta) \geq -3,
$$

and $\alpha \in [0, 2\pi)$ and $\theta \in [0, 2\pi)$. The set of a values for Equation 2.68 to be valid is as follows: $0.5248 \leq a \leq 0.8508$ and $-0.8508 \leq a \leq -0.5248$. By using the normalization condition, the range for b can be easily found: $0.5254 \leq b \leq 0.8512$. For $b \leq 0$, one can get the same results for a and $-0.5254 \geq b \geq -0.8512$. Any qutrit state with coefficients inside these ranges can not violate the KCBS inequality independent of Euler rotation angles; however, for the excluded a and b values, one may observe contextuality by finding five measurement bases through rotations.

We checked the specific qutrit states of the real Hilbert space and categorized them in terms of contextuality through rotational analysis. The classification of quantum systems of all kinds is an important issue, and our work is a step toward this goal. Our technique can be experimentally realized with current technology.

2.4 The Violation of the Monogamy Relation Between Non-locality and

Contextuality

In this chapter, we will discuss the monogamy relation observed between non-local and contextual characteristics in qutrit systems. The simple definition of the monogamy relation is the constraint on two aspects of observable quantumness, non-locality and contextuality. Observing one of them means the lack of observation for the other.

Monogamy has been observed between non-locality and contextuality (Kurzyński et al., 2014), which has been realized later (Zhan et al., 2016). In this scenario, one observes the violation of one inequality while there is no violation of the other. For example, if one observes the violation of the CHSH inequality, i.e., a quantum system exhibits non-local behavior for a given state, then it does not violate the KCBS inequality; in other words, it is a non-contextual state.

Let us look at the scenario where we observe this monogamy: We have two observers, Alice and Bob, sharing pairs of quantum systems. Alice performs five cyclic measurements from the KCBS scenario, denoted by A_i in Equation 2.30. Recall that A_i and A_{i+1} are compatible measurements. Each measurement has two possible outcomes, -1 and $+1$. Alice chooses two compatible observables while Bob selects only one of two incompatible measurements B_1 or B_2. There are two possible outcomes, -1 and $+1$, just like Alice's outcomes. In total, there are seven
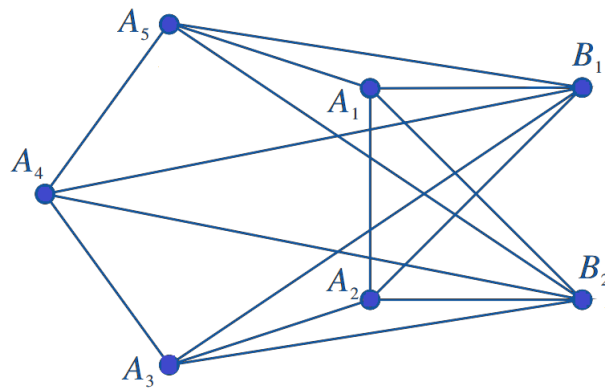
Figure 2.8 Compatibility among the measurements selected for both the KCBS and CHSH scenarios, and to show the monogamy relation between them. $A_1, ..., A_5$ are the measurements selected by Alice, forming the KCBS pentagram. B_1 and B_2 are selected by Bob for the CHSH scenario. Vertices are measurements, and the lines connecting them represent compatibility between pairs. This figure is adapted from (Kurzyński et al., 2014).

measurements, two of which are selected for both the KCBS and CHSH inequalities. Their compatibility relations can be seen in Figure 2.8. The violation of the KCBS inequality restrains the violation of the CHSH inequality, or vice versa. There is a trade-off between the different aspects of a quantum system. This implies there is a certain limit to quantumness. The generalization of monogamy had been of great importance and had been yet to be proven explicitly. Therefore, one should ask whether it is a fundamental relation. Along this direction, the monogamy relation has been tested, and polygamy between these properties is observed (Xiao et al., 2022). We will look at a two-qutrit quantum system.

Recall that the CHSH inequality is

$$-2 \leqslant \langle A_1 B_1 \rangle + \langle A_1 B_2 \rangle + \langle A_2 B_1 \rangle - \langle A_2 B_2 \rangle \leqslant +2$$

where

$$A_1 = Z, \quad A_2 = X,$$
$$B_1 = -(Z+X)/\sqrt{2}, \quad B_2 = (Z-X)/\sqrt{2},$$

and also

$$X = \begin{pmatrix} 0 & 1 \\ 1 & 0 \end{pmatrix}, Z = \begin{pmatrix} 1 & 0 \\ 0 & -1 \end{pmatrix}.$$

The maximal violation of the CHSH inequality requires maximal entanglement of a two-qubit state. It is possible to observe the maximal violation in a proper subspace of qutrits. To do this, one defines effective two-qubit states by making use of the following bases,

$$|1\rangle = \begin{pmatrix} 1 \\ 0 \\ 0 \end{pmatrix}, |0\rangle = \begin{pmatrix} 0 \\ 1 \\ 0 \end{pmatrix}, |-1\rangle = \begin{pmatrix} 0 \\ 0 \\ 1 \end{pmatrix}.$$

These are eigenstates of spin-1 operator to define new bases, $|0\rangle$ and $|+\rangle$ ($|+\rangle = (|1\rangle + |-1\rangle)/\sqrt{2}$). We consider the following quantum state,

$$\begin{aligned} |B_1\rangle &= a\,|00\rangle + b\,|++\rangle \\ &= a\,|00\rangle + b\Big[\frac{1}{\sqrt{2}}(|1\rangle + |-1\rangle) \otimes \frac{1}{\sqrt{2}}(|1\rangle + |-1\rangle)\Big] \\ &= a\,|00\rangle + \frac{b}{2}(|11\rangle + |1,-1\rangle + |-1,1\rangle + |-1,-1\rangle). \end{aligned}$$

(2.69)

We define the effective Pauli operators, X' and Z', which leads to

$$(2.70) \quad \begin{aligned} S_{CHSH} &= Z' \otimes \frac{-(Z'+X')}{\sqrt{2}} + Z' \otimes \frac{Z'-X'}{\sqrt{2}} \\ &+ X' \otimes \frac{-(Z'+X')}{\sqrt{2}} + X' \otimes \frac{Z'-X'}{\sqrt{2}} \end{aligned}$$

where

$$(2.71) \quad Z' = \begin{pmatrix} -1 & 0 & 0 \\ 0 & 1 & 0 \\ 0 & 0 & -1 \end{pmatrix}, \quad X' = \begin{pmatrix} 0 & \frac{1}{\sqrt{2}} & 0 \\ \frac{1}{\sqrt{2}} & 0 & \frac{1}{\sqrt{2}} \\ 0 & \frac{1}{\sqrt{2}} & 0 \end{pmatrix}.$$

The eigenvalues of the effective Pauli matrices, X' and Z', are $+1$ and -1, which are the same as the eigenvalues of the usual Pauli matrices. The average value of the CHSH operator is found as:

$$(2.72) \quad \langle B_1 | S_{CHSH} | B_1 \rangle = -\sqrt{2}|a+b|^2$$

When a and b are taken $\frac{1}{\sqrt{2}}$, the expectation value of the CHSH operator is $-2\sqrt{2}$ which is the maximum quantum value, i.e., the maximal violation of the CHSH inequality.

We can form the KCBS inequality by using the new bases, and five measurement bases are determined accordingly. The z-axis is orthogonal to pentagram plane (Klyachko, 2002; Klyachko et al., 2008). We obtain the average of the KCBS operator as follows:

$$(2.73) \quad \langle S_{KCBS} \rangle = \left(5 - 4\sqrt{5}\right)|a|^2 + \left(2\sqrt{5} - 5\right)|b|^2$$

Nine measurements are performed, four of which are for the CHSH scenario, whereas the others are the five cyclic measurements for the KCBS test. Unlike (Kurzyński et al., 2014), one does not use measurement bases common to both tests. Kurzyński et al. have shown that there is a trade-off between the violations of both inequalities; in other words, if one observes a violation of one of the inequalities, the other inequality is not violated, giving results within the classical range (Kurzyński et al., 2014). This approach is based on the No-disturbance principle which is satisfied by QT. As mentioned earlier, in the scenario proposed by Kurzyński et al., Alice and Bob perform measurements on a qutrit- and qubit-system, respectively. Alice aims to observe the contextual nature of qutrits, and she and Bob try to find non-local quantum states violating the CHSH inequality. In total, there are seven measurements. The CHSH test includes four measurements, two of which are se-

41
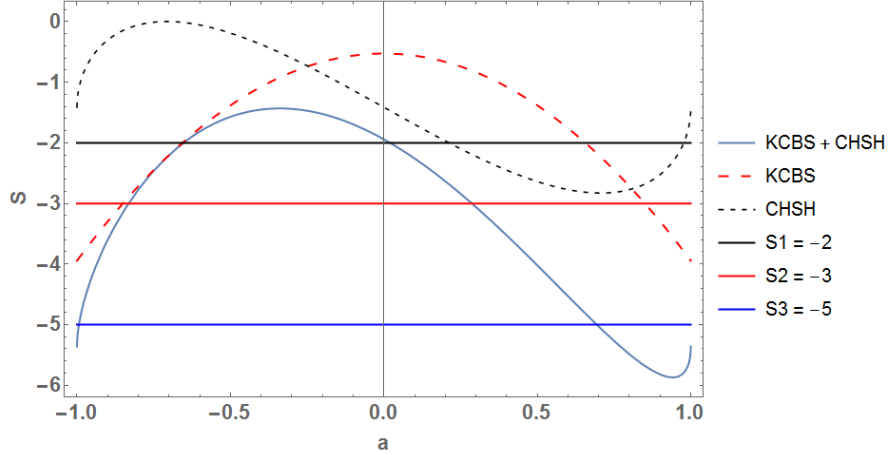
Figure 2.9 ($1 \geq b \geq 0$, $1 \geq a \geq -1$) The expectation values of the CHSH and KCBS operators and their sum. The classical bounds are also shown just to see the violations of both inequalities. All these measurements are performed in a two-qutrit quantum state. The summation of $\langle S_{CHSH} \rangle$ and $\langle S_{KCBS} \rangle$ exceeds the lower limit, -5, which is not in agreement with the monogamy relation.

lected among the KCBS measurements, provided that these are incompatible with each other. The authors ask whether the monogamy relation always holds (Xiao et al., 2022). To answer this, one finds the sum of Equations 2.72 and 2.73 where a and b are taken as real numbers,

$$(2.74) \quad \mathbb{S} = \langle S_{CHSH} \rangle + \langle S_{KCBS} \rangle = -\sqrt{2}(a+b)^2 + \left(5 - 4\sqrt{5}\right)a^2 + \left(2\sqrt{5} - 5\right)b^2.$$

b is a nonnegative real number, and due to the normalization condition, we are allowed to write $\mathbb{S}$ as a function of a as seen in Figure 2.9. $\langle S_{CHSH} \rangle$ and $\langle S_{KCBS} \rangle$ are lower than their respective bounds for some range of a, which means both inequalities are violated; in other words, there is no monogamy. In Figure 2.10, one can see the plot with $-1 \leq b \leq 0$.

We looked into the subspace of two-qutrit states and, by using appropriate matrices, we have seen the violation of the CHSH inequality. We applied the KCBS operator on the states of the same subspace, and the expectation value of the KCBS operator was found. We used independent observables, i.e., there is no common measurement to both tests. We observed simultaneous violation of both tests; in other words, the monogamy relation does not hold after choosing independent measurements (Xiao et al., 2022).

One can also observe the violation of the monogamy relation for the two-qutrit state,

$$(2.75) \quad |B_2\rangle = a\left(|0\rangle \otimes \frac{1}{\sqrt{2}}\left(|1\rangle + |-1\rangle\right)\right) + b\left(\frac{1}{\sqrt{2}}\left(|1\rangle + |-1\rangle\right) \otimes |0\rangle\right)$$

42
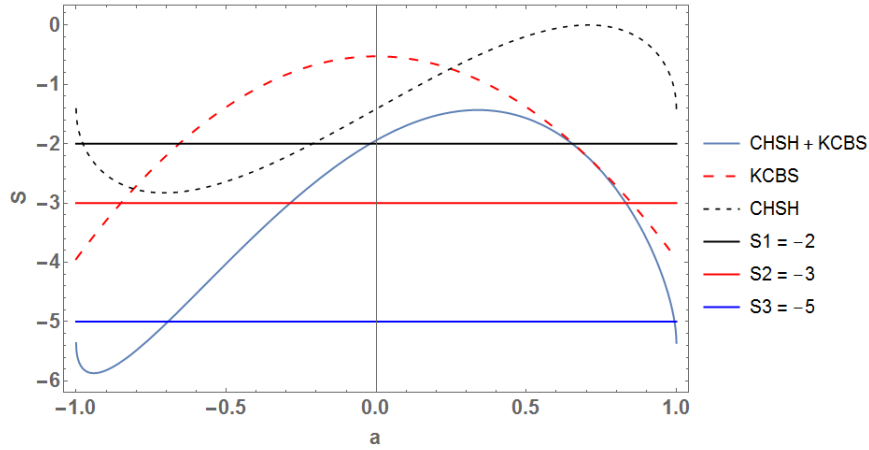
Figure 2.10 The same plot as illustrated in Figure 2.9 except that the sign of b values are minus here. $(0 \geq b \geq -1)$.

which can be rewritten as an effective two-qubit state,

$$(2.76) \qquad\qquad |B_2\rangle = a|0+\rangle + b|+0\rangle.$$

a and b values are real again, and the above state is tested. One gets the average values of both KCBS and CHSH operators plotted in Figures 2.11 and 2.12.

Both inequalities can be violated for a qutrit-qubit system. In this case, one should use the usual Pauli spin operators X and Z for a qubit. Since X' and Z' are the effective Pauli matrices which give the same eigenvalues as the usual Pauli operators,
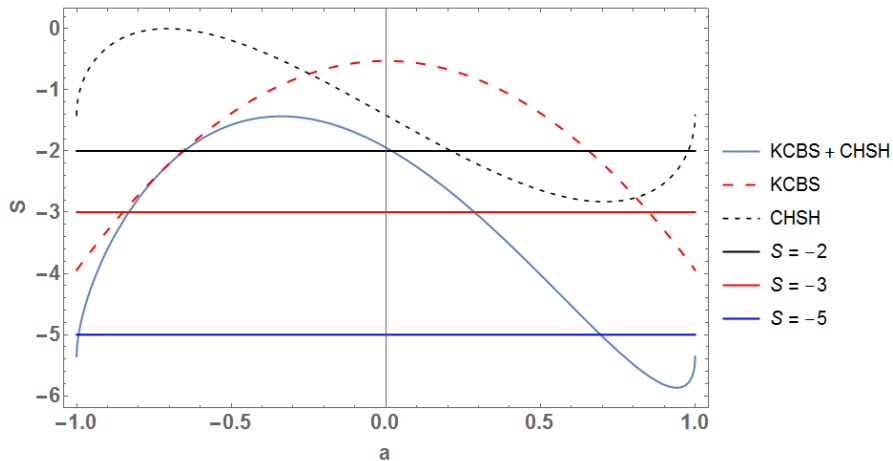
Figure 2.11 $(1 \geq b \geq 0, 1 \geq a \geq -1)$ The plots of the expectation values of KCBS and CHSH operators for given a and b values. One performs the same measurements on a two-qutrit state with different coefficients. Classical lower bounds for non-contextuality and locality are shown so that dual violation can be seen. As can be seen in the figure, there are contextually non-local states, which means the monogamy relation is not always valid.

43
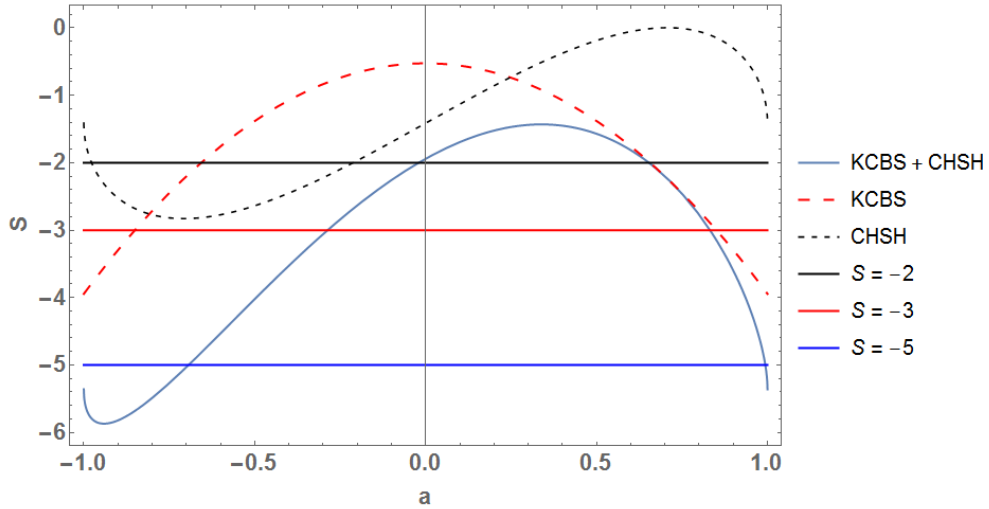
Figure 2.12 $(0 \geq b \geq -1)$ The similar plot as Figure 2.11 but the only difference is that b takes negative values.

and probabilities purely depend on the coefficients, a and b, the expectation value of S_{CHSH} will be identical. Also, the plots will be the same as well. The main difference between the scheme in (Kurzyński et al., 2014) and the current proposal is that one uses nine measurements, none of which is common to both tests. In contrast, two measurements from the CHSH scenario are chosen among the KCBS measurements in (Kurzyński et al., 2014). We illustrated this difference in the graphs from Figure 2.13.

In this chapter, we looked into a two-qutrit system for both inequalities. We saw that there are contextually non-local quantum states (Xiao et al., 2022). In (Kurzyński et al., 2014), two measurements are chosen from the KCBS scenario to test the CHSH inequality, and this restriction is the main cause of the monogamy relation. The trade-off between KCBS and CHSH violations is not necessarily fundamental, which depends on the measurement scenario. In conclusion, it is impossible to generalize the monogamy relation to any measurement scenario (Xiao et al., 2022).

2.5 Mathematical Relation between Contextuality and Entanglement

Quantum contextuality and non-locality are fundamental concepts of Quantum Theory and have been a hot topic since the pioneering works (Gleason, 1957; Bell, 1966; Specker, 1960; Kochen & Specker, 1967). We need to understand these concepts to

have a better idea of the governing dynamics in Quantum Theory. Finding possible correlations in various quantum systems is essential such that it may lead us to realize the differences between quantum physics and the classical world. Non-locality and contextuality are still under debate among the scientific community. The hidden variables could have been the reason underlying these concepts; however, this possibility has later been denied by various works (Bell, 1966; Specker, 1960; Kochen & Specker, 1967; Bell, 1964; Aspect et al., 1982; Freedman & Clauser, 1972). As mentioned earlier, the Bell inequality and the KCBS inequality (Bell, 1966; Klyachko, 2002, 2007; Binicioğlu et al., 2007; Klyachko et al., 2008) are the simplest examples including four and five measurements, respectively. These are the measurement scenarios where we observe non-locality and contextuality by using as least measurements as possible. In this chapter, we will mainly discuss the KCBS inequality where qutrit states (three-level quantum systems) are used, and spin-1 measurements are performed. Some qutrit states exhibit contextual behavior intrinsically and are compatible with quantum predictions without entanglement (Ahrens et al., 2013; Łapkiewicz et al., 2011). As discussed earlier, quantum contextuality can be observed for every qutrit state when more measurements are performed (Kurzyński & Kaszlikowski, 2012; Yu & Oh, 2012).

The outline of this section is as follows: First, we will discuss the KCBS inequality
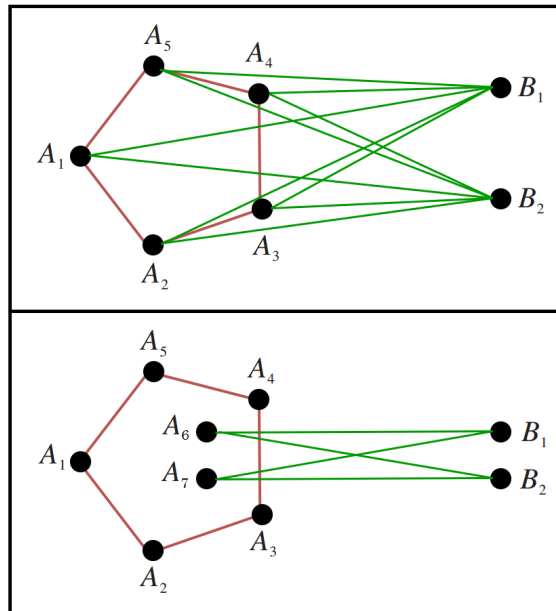
Figure 2.13 The top-side figure, including vertices and lines, is the graph for the compatibility of the measurements in the monogamy scenario (Kurzyński et al., 2014). Vertices represent measurements, and adjacent vertices show that they are compatible with each other. On the bottom, one can see the compatibility graph of the current scenario. There are nine measurements in total, none of which is common to both tests.

to recall it and what its violation means. Later, Majorana Stellar Representation (MSR) will be introduced (Majorana, 1932; Bloch & Rabi, 1945; Mäkelä & Messina, 2010), and we will apply it to define effective qutrits corresponding to symmetric two-qubit systems. MSR is in use for mutually unbiased basis (MUB)s and symmetric informationally complete positive operator valued measure (SIC-POVM)s (Aravind, 2017). The qutrits of MSR will be investigated using the KCBS operator (Diker & Gedik, 2022). Furthermore, we will find the concurrence (Wootters, 2001) for two-qubit systems and its relation with the average value of the KCBS operator (Klyachko, 2002, 2007; Binicioğlu et al., 2007; Klyachko et al., 2008; Diker & Gedik, 2022). The next step will be to derive the formula of the maximal contextuality when concurrence is known (Diker & Gedik, 2022). This will allow us to find the relation between the maximal non-locality and contextuality by comparing the KCBS scenario with the CHSH scenario (Diker & Gedik, 2022). When there is no entanglement, we will see that the outcomes of measurements do not exceed a limit (Diker & Gedik, 2022). How entanglement and contextuality are in connection for the KCBS scenario will be seen explicitly (Diker & Gedik, 2022). Lastly, we will divide qutrits based on their violations of the classical bounds (Diker & Gedik, 2022).

The action of an observer affects the observation in quantum physics, which differs it from classical physics. This involvement affects the outcome of a measurement. This is not in agreement with the locality principle. According to QT, a particle does not reveal its properties independent of observation. What you observe is not the state in which a particle was. Local restrictions are not valid anymore. As mentioned before, Bell has tested locality and has seen that some quantum systems are independent of local restrictions (Bell, 1966). Later, it has been shown that any entangled state is capable of violating the locality inequality (Gisin, 1991). The violation of the Bell inequality is observed in a 4-dim Hilbert space. The next step was to show whether one can find an inequality that can be violated in a Hilbert space with less than 4 dimensions. Kochen and Specker have succeeded in observing non-classicality in a 3-dim Hilbert space (Specker, 1960; Kochen & Specker, 1967). This is called contextuality, defined uniquely for quantum physics.

The KCBS test (Klyachko, 2002, 2007; Binicioğlu et al., 2007; Klyachko et al., 2008), which is the simplest contextuality scenario, has been discovered. We discussed it earlier in detail. To recall the KCBS inequality, let us give it again:

$$\langle A_1 A_2 \rangle + \langle A_2 A_3 \rangle + \langle A_3 A_4 \rangle + \langle A_4 A_5 \rangle + \langle A_5 A_1 \rangle \geq -3,$$

which is a state-dependent non-contextuality inequality. S_i are the usual spin-1

operators and

$$A_i = 2S_i^2 - 1.$$

The directions of S_i and S_{i+1} are perpendicular to each other, allowing us to measure A_i and A_{i+1} together. We obtain the results outside the classical range; in other words, qutrit states exhibit contextuality and do not have to be entangled with any quantum system. The maximal violation of the KCBS inequality is observed for the neutrally polarized spin state $|0\rangle$. They have found the quantum lower limit close to -4 ($\cong -3,94$).

2.5.1 Concurrence and the expectation value of the KCBS operator

It has been shown that a qutrit can be intrinsically entangled (Can et al., 2005). The symmetric group of two-qubit states has been investigated and written as effective qutrits for which the concurrence inequality has been found (Binicioğlu et al., 2007).

We will use MSR for the symmetric two-qubit states to rewrite them as effective qutrits. The symmetric set of two-qubit states violating the KCBS inequality has already been found (Soeda et al., 2013). We aim to do the same using the MSR. We take advantage of the MSR representation to work with the whole group of qutrits. MSR of any qubit can be seen as a vector from the origin to a point on the Bloch sphere. The subgroup of symmetric two-qubit states is needed in our case. A symmetric two-qubit state represented in MSR can be expressed as follows:

$$(2.77) \qquad |\psi\rangle = \frac{1}{N}(|m\rangle|n\rangle + |n\rangle|m\rangle)$$

where

$$(2.78) \qquad |m\rangle, |n\rangle = (\cos\frac{\theta_{1,2}}{2} \quad \sin\frac{\theta_{1,2}}{2}e^{i\phi_{1,2}}).$$

The matrix representation of the state in Equation 2.77 is as follows:

$$(2.79) \qquad |\psi\rangle = \frac{1}{2N}\begin{pmatrix} 2\cos\left(\frac{\theta 1}{2}\right)\cos\left(\frac{\theta 2}{2}\right) \\ e^{i\phi 1}\cos\left(\frac{\theta 2}{2}\right)\sin\left(\frac{\theta 1}{2}\right) + e^{i\phi 2}\cos\left(\frac{\theta 1}{2}\right)\sin\left(\frac{\theta 2}{2}\right) \\ e^{i\phi 1}\cos\left(\frac{\theta 2}{2}\right)\sin\left(\frac{\theta 1}{2}\right) + e^{i\phi 2}\cos\left(\frac{\theta 1}{2}\right)\sin\left(\frac{\theta 2}{2}\right) \\ 2e^{i(\phi 1+\phi 2)}\sin\left(\frac{\theta 1}{2}\right)\sin\left(\frac{\theta 2}{2}\right) \end{pmatrix}$$

Symmetric two-qubit states can be rewritten as effective qutrits (Can et al., 2005).

The state $|\psi\rangle$ is a symmetric one, so we can express it as a qutrit:

$$\text{(2.80)} \qquad |\psi^*\rangle = \frac{1}{N}\begin{pmatrix} \cos\frac{\theta_1}{2}\cos\frac{\theta_2}{2} \\ \frac{1}{\sqrt{2}}(e^{i\phi_1}\cos\frac{\theta_2}{2}\sin\frac{\theta_1}{2} + e^{i\phi_2}\cos\frac{\theta_1}{2}\sin\frac{\theta_2}{2}) \\ e^{i(\phi_1+\phi_2)}\sin\frac{\theta_1}{2}\sin\frac{\theta_2}{2} \end{pmatrix}$$

where

$$\text{(2.81)} \qquad N = \sqrt{\frac{1}{4}(\sin\theta_1\sin\theta_2\cos(\phi_1-\phi_2)+\cos\theta_1\cos\theta_2+3)}.$$

We calculate the average of the KCBS operator, which gives the following:

$$\text{(2.82)} \qquad \langle\psi^*|\mathbb{S}_{KCBS}|\psi^*\rangle = \frac{4\left(3\sqrt{5}-5\right)(\cos\theta_1\cos\theta_2+1)}{\sin\theta_1\sin\theta_2\cos(\phi_1-\phi_2)+\cos\theta_1\cos\theta_2+3} + (5-4\sqrt{5}).$$

We obtain a function of θ_1, θ_2 and $\Delta\phi$ where

$$\text{(2.83)} \qquad \Delta\phi = \phi_1 - \phi_2.$$

One may denote the average of the KCBS operator as follows: $S = \langle\psi^*|\mathbb{S}_{KCBS}|\psi^*\rangle$. In Figure 2.14, the distinction between contextuality and non-contextuality regions is shown in a 3-dim plot. We find the numeric part of the right-hand side in Equation 2.82 equal to the quantum lower limit ($\cong -3,94$), i.e., we observe the maximal violation of the KCBS equality. Since that part is the lowest value possible in QT, we can see that as a reference point for the determination of the degree of contextuality (recall that, for classical measurements, we obtain -3 as the classical lower limit).

Next, we will find the concurrence of two-qubit states, which will give us the measure of self-entanglement for effective qutrits (Wootters, 2001). For two-qubit states given in the general form as below:

$$\text{(2.84)} \qquad |\Psi\rangle = a\,|00\rangle + b\,|01\rangle + c\,|10\rangle + d\,|11\rangle,$$

we use the following formula to find concurrence:

$$\text{(2.85)} \qquad C = 2|ad - bc|.$$

We apply this to our symmetric two-qubit states given in Equation 2.79 and get

$$\text{(2.86)} \qquad C(\theta_1,\theta_2,\Delta\phi) = \frac{1-\cos\theta_1\cos\theta_2-\cos\Delta\phi\sin\theta_1\sin\theta_2}{3+\sin\theta_1\sin\theta_2\cos\Delta\phi+\cos\theta_1\cos\theta_2}.$$

This can be rewritten as:

$$(2.87) \qquad C[f(\theta_1, \theta_2, \Delta\phi)] = \frac{1 - f(\theta_1, \theta_2, \Delta\phi)}{3 + f(\theta_1, \theta_2, \Delta\phi)}.$$

The function $f(\theta_1, \theta_2, \Delta\phi)$ is a trigonometric function which is

$$(2.88) \qquad f(\theta_1, \theta_2, \Delta\phi) = \sin\theta_1 \sin\theta_2 \cos\Delta\phi + \cos\theta_1 \cos\theta_2.$$

We can define Equation 2.88 as follows:

$$(2.89) \qquad f(\theta_1, \theta_2, \Delta\phi) = \cos 2\theta_{mn},$$

and θ_{mn} corresponds to the angle between state vectors, $|m\rangle$ and $|n\rangle$. We can rewrite Equation 2.86 in terms of θ_{mn},

$$(2.90) \qquad C(\theta_1, \theta_2, \Delta\phi) = \frac{1 - \cos 2\theta_{mn}}{3 + \cos 2\theta_{mn}}.$$

The concurrence depends on the relative angle between these state vectors, $|n\rangle$ and $|m\rangle$. We may write Equation 2.88,

$$(2.91) \qquad f(\theta_1, \theta_2, \Delta\phi) = \frac{1 - 3C(\theta_1, \theta_2, \Delta\phi)}{1 + C(\theta_1, \theta_2, \Delta\phi)}.$$

One may define Equation 2.82 using $f(\theta_1, \theta_2, \Delta\phi)$ as in the following:

$$(2.92) \qquad S(\theta_1, \theta_2, \Delta\phi) = \frac{4\left(3\sqrt{5} - 5\right)(\cos\theta_1 \cos\theta_2 + 1)}{f(\theta_1, \theta_2, \Delta\phi) + 3} + \left(5 - 4\sqrt{5}\right)$$

When we use Equation 2.91 to redefine Equation 2.82, we obtain the following relation between concurrence and the average of the KCBS operator:

$$
\begin{aligned}
(2.93) \qquad S(\theta_1, \theta_2, \Delta\phi) &= \frac{4\left(3\sqrt{5} - 5\right)(\cos\theta_1 \cos\theta_2 + 1)}{\frac{1 - 3C(\theta_1, \theta_2, \Delta\phi)}{1 + C(\theta_1, \theta_2, \Delta\phi)} + 3} + \left(5 - 4\sqrt{5}\right) \\
&= \left(3\sqrt{5} - 5\right)(C(\theta_1, \theta_2, \Delta\phi) + 1)(\cos\theta_1 \cos\theta_2 + 1) + 5 - 4\sqrt{5},
\end{aligned}
$$

which may be rewritten as:

$$(2.94) \qquad S(\theta_1, \theta_2, \Delta\phi) = \left(3\sqrt{5} - 5\right)\left(\frac{1 - \cos 2\theta_{mn}}{3 + \cos 2\theta_{mn}} + 1\right)(\cos\theta_1 \cos\theta_2 + 1) + 5 - 4\sqrt{5}.$$

We have obtained the direct relation between concurrence and contextuality. Since concurrence depends on θ's and $\Delta\phi$, other cosine terms are correlated with concurrence. One can clearly see that the cosine terms make Equation 2.93 more compli-
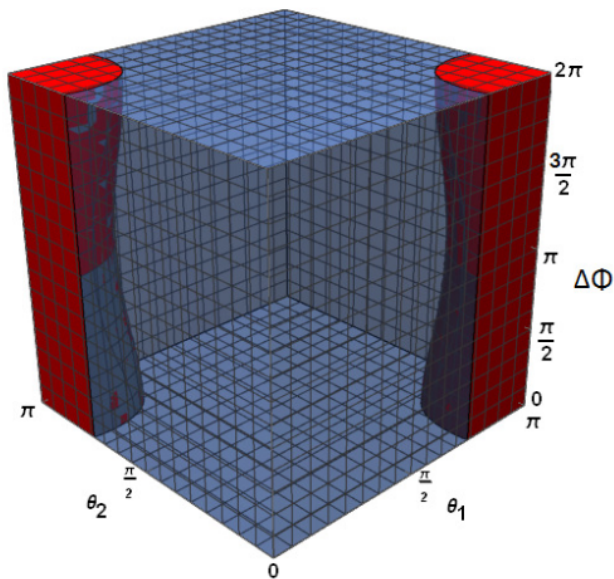
Figure 2.14 The illustration of (non-)contextuality regions for the S function defined as $S(\theta_i, \Delta\phi)$ $(i=1,2)$. The red part corresponds to the contextuality region $(S < -3)$; the blue translucent part is the region for the non-contextual states $(S > -3)$. We observe the maximum violation when $\theta_1 = 0$, $\theta_2 = \pi$ and $\theta_1 = \pi$, $\theta_2 = 0$ (the maximal contextuality of states does not depend on $\Delta\phi$). The two edges of the rectangular cuboid in the red region correspond to the maximal contextuality.

cated. Unfortunately, this is the neatest form one can write.

We will answer what happens to the S function when concurrence is known; in other words, for a given concurrence, we will give the degree of contextuality in the KCBS scenario. To do this, Equation 2.88 should not change so that concurrence is constant. Two variables$(\theta_{i=1,2})$ are correlated such that C is constant. The following condition provides that:

$$(2.95) \qquad \cos(\Delta\phi) = \frac{\frac{1-3C}{1+C} - \cos\theta_1\cos\theta_2}{\sin\theta_1\sin\theta_2},$$

and $-1 \leq \cos(\Delta\phi) \leq 1$. In Equation 2.93, the coefficient of the part containing cosine terms is above zero. θ values should be adjusted to make the cosine part as small as possible because we want to find the lowest value of the S function when concurrence is given. We will find the limit for $\theta_1 \to 0$ and $\theta_2 \to \pi$, or vice versa due to the symmetry between θs. It is obvious that

$$(2.96) \qquad \lim_{\substack{\theta_1 \to 0 \\ \theta_2 \to \pi}} \cos(\Delta\phi) = \pm\infty,$$

which does not make sense due to trigonometric restrictions. One needs to find the set of θ values for the upper and lower limits for Equation 2.95 $(-1 \leq \cos(\Delta\phi) \leq 1)$.

When $\cos(\Delta\phi) = \pm 1$, we find that

$$(2.97) \qquad \cos^{-1}\left(\frac{1-3C}{1+C}\right) = \theta_1 - \theta_2$$

and

$$(2.98) \qquad \cos^{-1}\left(\frac{1-3C}{1+C}\right) = \theta_1 + \theta_2.$$

We make use of these relations to express θ_1 in terms of θ_2 and concurrence. Recall that the expectation value of the KCBS operator, $S(\theta_1, \theta_2, \Delta\phi)$ has three degrees of freedom. Since θs can be defined in terms of each other and concurrence is taken to be constant, reducing the number of variables is possible, leaving us with only one parameter. The S function has only one variable $(S(\theta_i))$. Notice that we look into the case for the minimum of $S(\theta_i)$ when $\cos(\Delta\phi) = \pm 1$. Next, one solves for $dS(\theta_2)/d\theta_2 = 0$ and finds the following solutions:

$$(2.99) \qquad \theta_2 \in \left\{ \frac{1}{2}\left(\pi + \cos^{-1}\left(\frac{1-3C}{1+C}\right)\right), \frac{1}{2}\left(\pi - \cos^{-1}\left(\frac{1-3C}{1+C}\right)\right) \right\}.$$

This gives us the following:

$$(2.100) \qquad S_{KCBS}^{min} = \left(5 - 3\sqrt{5}\right)C - \sqrt{5}.$$

This gives the lower bound of the S function when concurrence is known. Equation 2.100 shows us the degree of violation of the KCBS inequality for a given concurrence. This is a simple linear relation between contextuality and the degree of entanglement. We know that

$$(2.101) \qquad 0 \le C \le 1.$$

For $C = 0$,

$$(2.102) \qquad S_{KCBS}^{min} = -\sqrt{5}$$

which is the lower bound for locally-defined states. We obtain the classical lower bound imposed by local restrictions, and the classical lower bound is shifted from -3 to $-\sqrt{5}$ and draws a clearer line between classicality and quantumness. For the cases when the outcomes of measurements are below this new limit, we see only non-local quantum states. For two maximally-entangled particles $(C = 1)$,

$$(2.103) \qquad S_{KCBS}^{min} = 5 - 4\sqrt{5}$$

which corresponds to the maximal contextuality for the KCBS scenario. The lower bound for non-contextuality is $S_{KCBS} = -3$, and this gives us

$$(2.104) \qquad\qquad C \cong 0.447.$$

That is not a small number considering that the upper limit for concurrence is one. Quantum states must be well entangled so that it is possible to observe quantum contextuality. This is a significant result for us to see the relation between contextuality and entanglement. Similarly, the CHSH inequality is maximally violated for a known concurrence according to the following equation:

$$(2.105) \qquad\qquad \beta = 2\sqrt{1 + C^2}.$$

One takes the average of the CHSH operator, which is β (Wootters, 1998; Verstraete & Wolf, 2002). The relation between the maximal violations of both inequalities is given in the following:

$$(2.106) \qquad\qquad S \propto -\sqrt{\beta^2 - 4}.$$

This is the direct relation between contextuality and non-locality for when they are as maximal as possible (concurrence is constant).

2.6 Quantum Correlations in the Delayed-Choice Experiment

In this section, we will discuss the delayed-choice experiment of which there are two versions: Wheeler's delayed-choice experiment (Wheeler et al., 1984; Wheeler, 1978) and the Quantum Delayed-Choice Experiment QDCE (Ionicioiu & Terno, 2011; Peruzzo et al., 2012). Then, we will mention the different version of the QDCE by using the polarization property of a photon instead of the spatial modes used in the original QDCE. Lastly, we will investigate quantum correlations in this experiment concerning entanglement and quantum contextuality. This will give readers an idea of how these fundamental concepts of Quantum Theory are related to the wave-particle duality.
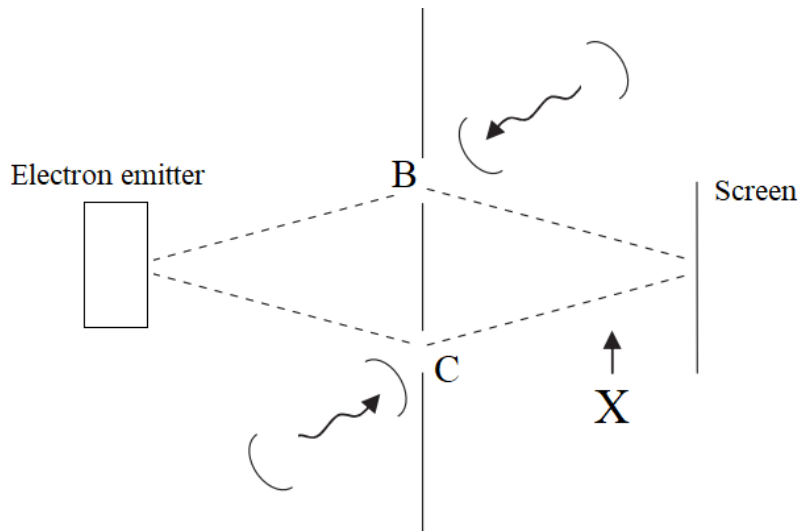
Figure 2.15 Young's slit experiment. One may or may not choose to observe if an electron goes through slit B or C. We use the brackets for the optionality of the observation

2.6.1 Wheeler's Delayed-Choice Experiment

The wave-particle duality is the fundamental concept of quantum mechanics and has been intriguing since its observation. In Figure 2.15, the standard Young's slits setup is shown, and we observe the usual interference pattern on the screen. This is the wave behavior of electrons used in this experiment. If electrons are detected on the intermediate slits, they take only one of the routes and go through one of the holes; in other words, they behave as a classical particle. In this case, they are observed on the specific spots of the screen, and no interference occurs. If photons are used instead of electrons, we observe the same duality. For photons, one removes the screen and uses a pair of detectors instead. We see that one detector or the other clicks but both of them never click simultaneously. One can see the setup for photons in Figure 2.16.

If the photon goes through Slit C, Detector 1 clicks. When Detector 2 clicks, it means that the photon came through B. Bohr concluded that whether one observes wave or particle properties of particles depends on the arrangement of the experimental apparatus. The arrangements for observing wave-like and particle-like properties are always mutually exclusive (*complementarity*). This can be easily seen in the example of the photon. We will discuss only the case of photons in this section.

Does the photon know in advance whether the arrangement has been made to observe the wave property (Figure 2.16) or the particle property? This question was asked (Weizsäcker, 1931) in the beginning stage of quantum mechanics, and in 1978
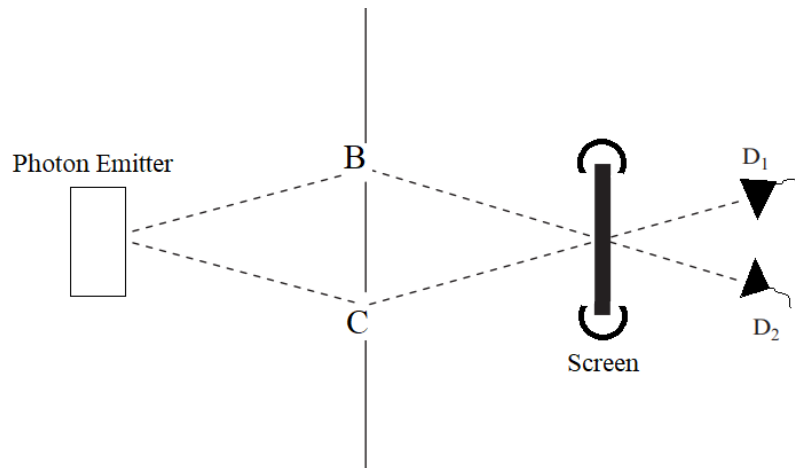
Figure 2.16 A setup where we observe "wave-particle duality" for photons. The brackets around the screen show that we may put it there (to observe the "wave" aspect) or remove it (to observe the "particle" aspect)

John Archibald Wheeler showed that one can answer this question by setting up an experiment in which we decide which configuration to use until after the photon is within the apparatus (Wheeler et al., 1984; Wheeler, 1978). We call this experiment a "delayed-choice" experiment since the decision is made later when the photon is already inside the apparatus. Several have been demonstrated over the last three decades using not only photons but also neutrons and atoms. The choice of configuration in advance or only at the last moment does not change the counting statistics.

When photons are used, and the lengths of the apparatus are taken in the order of 3 m, the time needed for a photon to transit is about 10 ns. So we need to make the choice in a time shorter than this. This makes it impossible to insert or remove a screen as in Figure 2.16; however, by using the polarization degree of photons, one can get rid of this difficulty. One needs to correlate (or decline to correlate) the path with the polarization of a photon. A choice is made over a few nanoseconds using a device such as a Pockels cell. The plane of polarization is rotated by 90° using this device.

A schematic realization of the experiment is given in Figure 2.17. The source emits the photons which are polarized in the plane of the paper, and when there is not the Pockels cell (or not activated), both beams are polarized throughout the experiment. At BS2, they interfere with a relative phase, and the relative phase is controlled by the phase shifter. Thus, under these conditions provided by the apparatus, we see that the output of the Detector 1 depends on the phase difference introduced by the shifter. The phase difference corresponds to the wave behavior of the photons. If we activate the Pockels cell, we rotate the polarization of a photon in the lower
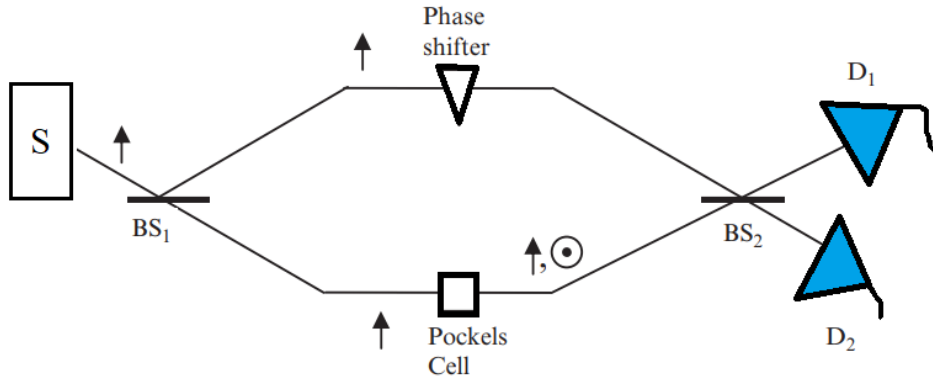
Figure 2.17 The polarization-mediated delayed-choice experiment. The notation after the Pockels cell shows both choices: the direction of polarization may be either out-of-plane or in-plane.

beam, so it is perpendicular to the polarization of the other beam. In this case, we use polarization for labeling the path taken by a given photon. This means no interference at BS2 assumed to be polarization insensitive. The output of detector Detector 1 is equal to the sum of what we would find for each of the two beams separately; because the output does not depend on the position of the phase shifter, the total output of Detector 1 with the activated Pockels cell is not affected by the latter (*particle* property). One should notice that the cell can be activated after the splitting of the photon wave packet at Beam Splitter 1 (BS1).

Over the last two decades, a number of experiments have been demonstrated. One of them is the most similar to Wheeler's original experiment (Jacques et al., 2007), in which a setup similar to that of Figure 2.17 is used. In this work, the interferometer length was 48 m, and a quantum random number generator (QRNG) decides whether or not to activate the switching cell. This decision is made close to the far end. After the photon has gone through the first beam splitter, it goes into the future light cone of the random choice event. We use QRNG to ensure that the photon can not know the choice in advance. When the wave configuration is realized for photons, and the output of one of the detectors depends on the phase shift between the two beams, one observes a sinusoidal plot with a visibility of 94%. If the particle configuration is realized, we observe the flat pattern.

It has been shown that there is an interesting variant of the "delayed-choice" experiment (Kim et al., 2000). In Figure 2.18, the schematic setup is illustrated. One prepares the source such that we have nonzero mutually coherent amplitudes for two photons to be generated consecutively by either of two parts, A and B. Before Photon 2 reaches BS1 or BS2, screen S registers Photon 1. We aim to detect any

photon only coming from source A(B) at Detector 3 (Detector 4); on the other hand, if a photon arrives in Detector 1 or Detector 2, it could have been emitted by either source. If photons 1 are selected when their partners 2 were detected in Detector 4, the distribution of the photons seen on screen S is flat. In other case, only those with partners detected in Detector 1 are selected. Then, one observes a fringe pattern with a complementary one for those with their partners clicking Detector 2. It may seem baffling because Photon 1 was detected on screen S before Photon 2 knew whether BS1/2 would transmit or reflect it and thus whether Detector 3/Detector 4 or Detector 1/Detector 2 would detect.

This is not a paradox; the results are very consistent with an application of quantum measurements. Let us give an example: we detect photon 1, and there is a node for the observed pattern for the Detector 1-correlated subensemble. The detection of the photon means that a (quasi-) macroscopic event has been induced by it, and the photon has been measured. If we perform the projection measurement on the two-photon system, we see that the amplitude of photon 2 is automatically zero, so everything makes sense. In the delayed-choice experiments, we observe the pitfalls of applying the projection measurement too early. At the same time, we have not seen anything macroscopically, and it is still possible to obtain a pattern of mutual interference of alternatives.
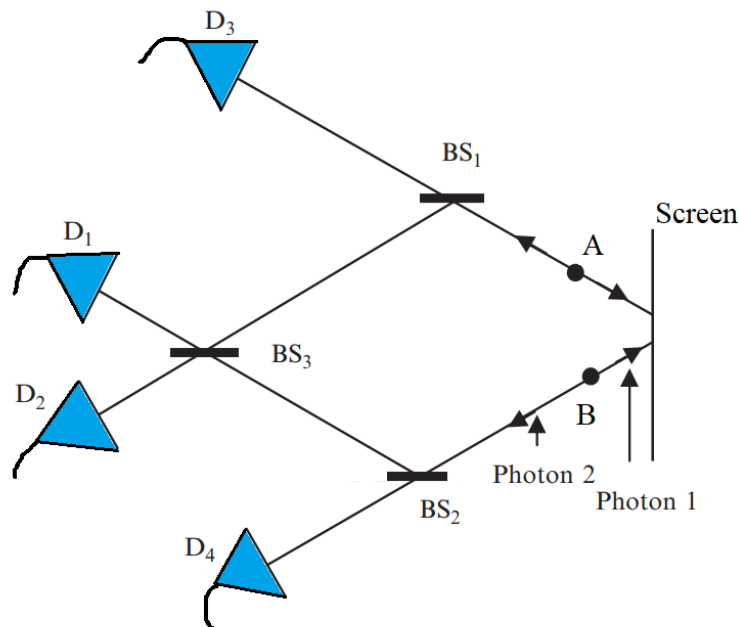
Figure 2.18 The setup proposed by Kim et al. (Kim et al., 2000)

56

2.6.2 The Quantum Delayed-Choice Experiment

Since the pioneering work by Einstein, Podolsky, and Rosen (Einstein et al., 1935), the quantum non-locality, which means that some physical quantities are independent of local restrictions defined in classical physics, has attracted the attention of the scientific community (Bell, 1966, 1964; Herbert & Karush, 1978; Heywood & Redhead, 1983; Stapp, 1982). The entanglement of quantum systems is directly related to non-locality, which made it possible to demonstrate the quantum delayed-choice experiment (QDCE) (Ionicioiu & Terno, 2011; Peruzzo et al., 2012). This is an adaptation of Wheeler's work concerning the notion of the wave-particle duality (Wheeler et al., 1984; Wheeler, 1978). Over the years, this duality has been discussed in detail by various researchers (Wheeler et al., 1984; Feynman et al., 1965; Scully et al., 1991; Englert, 1996); however, it had not been clear as to whether photons know beforehand how to act in specific measurement scenarios. Along this direction, Wheeler proposed a gedanken experiment (Wheeler et al., 1984; Wheeler, 1978) whose purpose is to test whether a photon behaves depending on a hidden variable. The result of this experiment is that a photon acts as a wave or particle, depending on how one arranges the experimental setup. Since the change in the setup is made while the photon goes through the interferometer, it cannot know beforehand what it will encounter. The delayed-choice experiment has been demonstrated in various setups (Hellmuth et al., 1987; Lawson-Daku et al., 1996; Kim et al., 2000; Zeilinger et al., 2005; Jacques et al., 2007; Manning et al., 2015).

Wheeler's proposal has been changed into a quantum optical version where photons reveal the particle and wave properties simultaneously by using a mode-based quantum circuit (Ionicioiu & Terno, 2011; Peruzzo et al., 2012). In this section, we will mainly discuss this approach and later introduce a polarization-based quantum circuit to show that the wave-particle duality is also observable using polarization-based photonic states.

The QDCE modifies Wheeler's approach and allows us to observe both the particle- and the wave-like properties of a photon with the help of an extra photon. On this circuit, we have a control-Hadamard gate (c-Had) acting as a two-qubit quantum gate whose transformations are in the following:

$$(2.107) \qquad cHad\,|10\rangle = |1\rangle \otimes \frac{1}{\sqrt{2}}(|0\rangle + |1\rangle),$$

and

(2.108)
$$cHad|11\rangle = |1\rangle \otimes \frac{1}{\sqrt{2}}(|0\rangle - |1\rangle).$$

States $|0\rangle$ and $|1\rangle$ are the spatial modes of a photon; in other words, they correspond to the paths taken by the photons. One can realize the c-Had gate by using nondeterministic phase gates (Ralph et al., 2002; Hofmann & Takeuchi, 2002). The detailed schematic depiction of the process is shown in Figure 2.19. The c-Had entangles two photons, which allows us to observe the wave-particle duality. There are two photonic states, one of which is the ancillary photon. Its state is given as

(2.109)
$$|\psi\rangle = \cos\alpha\,|0\rangle + \sin\alpha\,|1\rangle$$

where the system photon is in the state $|0\rangle$. The first gate is a single-qubit Hadamard gate which acts on the system photon,

(2.110)
$$Had|0\rangle = \frac{1}{\sqrt{2}}(|0\rangle + |1\rangle).$$

After this transformation, the global state of the system is

(2.111)
$$|\Psi_i(\alpha)\rangle = \frac{\cos\alpha}{\sqrt{2}}(|00\rangle + |01\rangle) + \frac{\sin\alpha}{\sqrt{2}}(|10\rangle + |11\rangle).$$

Then, we apply the phase shifter (P) to the system photon (denoted by $|\lambda\rangle$) giving us:

(2.112)
$$P|\lambda\rangle = \frac{1}{\sqrt{2}}(|0\rangle + e^{i\phi}|1\rangle).$$

We get an entangled biphotonic state after the c-Had gate acts on both photons. Hence, we obtain the final state as in the following:

(2.113)
$$\begin{aligned}\left|\Psi_f(\alpha,\phi)\right\rangle = {}&\cos\alpha\Big(\frac{1}{\sqrt{2}}(|0\rangle_s + e^{i\phi}|1\rangle_s)\Big)|0\rangle_a \\ &+ e^{i\phi/2}\sin\alpha\Big(\cos\frac{\phi}{2}|0\rangle_s - i\sin\frac{\phi}{2}|1\rangle_s\Big)|1\rangle_a,\end{aligned}$$

which gives information on both cases (whether the second beam splitter is absent or not). a and s correspond to the subspaces of the ancillary photon and the system photon, respectively. Using Equation 2.113, we find the intensity I_0 at detector D_0,

(2.114)
$$I_0(\alpha,\phi) = \frac{1}{2}\cos^2\alpha + \cos^2\frac{\phi}{2}\sin^2\alpha.$$

58

$|\psi\rangle = cos\alpha|0\rangle + sin\alpha|1\rangle$

$|0\rangle$ — H

Phase Shifter
φ

D_o
D_1
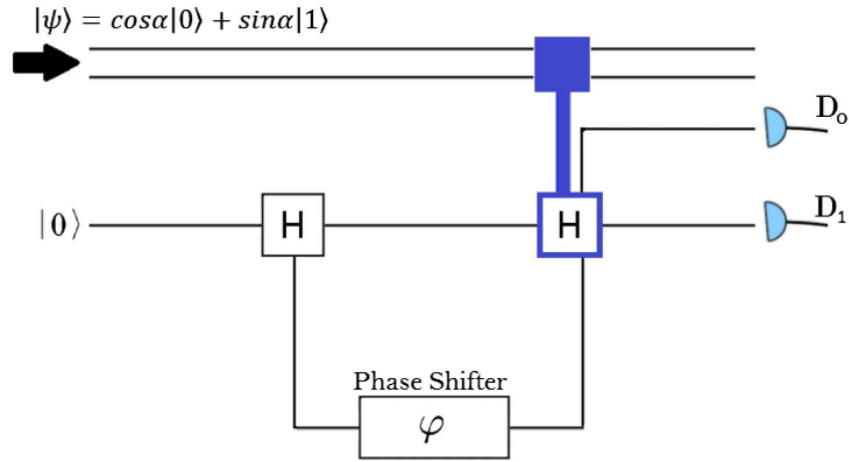
Figure 2.19 Ancillary photon, whose state is given in the top-left corner of the figure, goes into the circuit. The system photon, which is prepared to be in the state $|0\rangle$, also goes into the circuit. The operation of the Hadamard gate is realized by a beam splitter, giving us a superposition of two modes. Later on, we shift the phase for one of the modes so that we can observe the wave-like property at the end. Both the system photon and the ancillary photon go through the c-Had gate (shown in blue), after which we obtain the global state in Equation 2.113. Intensities at D_0 and D_1 depend on the relative amplitude (particle-like property) and the phase (wave-like property).

This naturally gives the intensity at detector D_1 as follows:

(2.115)
$$I_1 = 1 - I_0.$$

Both intensities depend on α and ϕ. Why is this important? We need to understand the physical meaning of these parameters in the context of QDCE. Since ϕ is the relative phase between two modes of the system photon, the intensities carry information on the wave-like property. Moreover, they depend on α as well; however, the state function of the system photon initially depends only on ϕ. The parameter α later comes from the interaction between the photons due to the action of c-Had gate. In other words, entangling two photons directly leads to the intensities affected by the particles' interaction. That is why the parameter α corresponds to the particle-like behavior. When the system photon is detected, we observe the wave- and particle-like properties of a photon.

2.6.2.1 The Polarization-based Quantum Delayed-Choice Experiment

In this subsection, we will propose a quantum circuit based on polarization transformation by modifying the original one to observe particle- and wave-like behaviors (Diker, 2018). Naturally, we make use of the polarization degree of freedom of a photon. The kets $|0\rangle$ and $|1\rangle$ are horizontally and vertically polarized photonic states. We aim to apply the same transformations and reach the same results regarding intensities (probability of detecting a photon). We make the following changes in the optical scheme: the role of first beam splitter in the original QDCE is given to a half-wave plate HWP. Two polarizing beam splitters PBSs and a phase shifter are used (Figure 2.20). After the first HWP act on the initial state $|H\rangle$, the system photon is transformed as follows:

$$(2.116) \qquad HWP|H\rangle = \frac{1}{\sqrt{2}}(|H\rangle + |V\rangle).$$

What a beam splitter does to mode states of a photon is done by the HWP to the polarization states. Horizontal and vertical polarizations are denoted by H and V, respectively. To add the wave property (phase) to the system photon, one needs to use a phase shifter between polarizations. Then, the photon is in a superposition of two paths by means of a PBS, on one of which we put a phase shifter. Here, the spatial mode, which is an extra degree of freedom of a photon, is temporarily created to shift the phase between the V and the H components of the system photon, giving us

$$(2.117) \qquad |\Psi^*\rangle = \frac{1}{\sqrt{2}}(|H\rangle|a\rangle + e^{i\phi}|V\rangle|b\rangle).$$

The kets $|a\rangle$ and $|b\rangle$ are the spatial modes, shown in Figure 2.20. These spatial modes allow us to perform the phase-shifting operation. The next HWP gets rid of the mode degeneracy, and the state of the system photon is

$$(2.118) \qquad |\Psi^{**}\rangle = \frac{1}{\sqrt{2}}(|H\rangle + e^{i\phi}|V\rangle).$$

Before the system photon is detected, the last operator c-Had, which is the main component of our circuit, acts on the two-photon state. As a result, the global state of the system of two photons (the ancillary photon and the system photon) is given
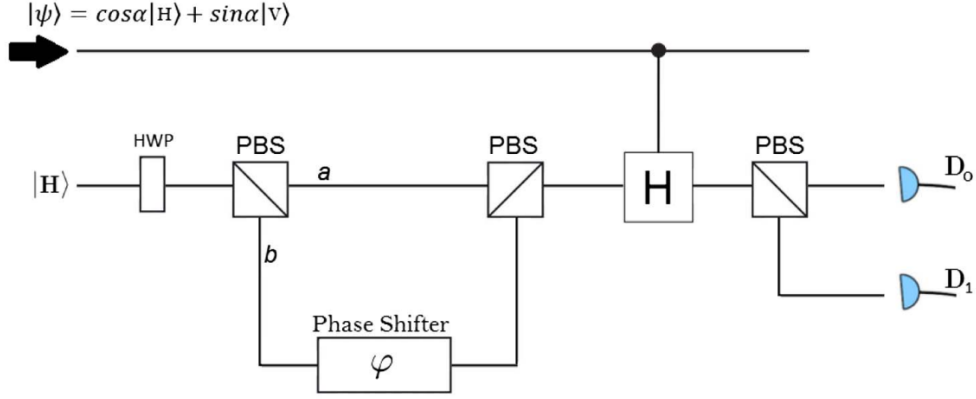
Figure 2.20 We send the system photon and the ancillary photon into the optical apparatus. On the top-left of the figure, the state of the ancillary photon is given, where angle α is set manually. HWP oriented at an angle $\frac{\alpha}{2}$ is used to obtain such a state. One can see that the system photon, which is horizontally polarized, is sent along the lower path. The first HWP at an angle $\frac{\pi}{8}$ corresponds to a Hadamard gate giving a superposition of two polarization states as output. The first PBS is used to create a temporary spatial mode; hence, we are able to shift the relative phase between these states. We get rid of the mode degeneracy by using the second PBS which combines pol-based photonic states. Later, the c-Had is used to entangle the ancillary photon with the system photon. Thus, one can observe both wave- and particle-like behaviors of the system photon. The last PBS divides the V- and H-polarized components into two modes so one can detect them separately.

as:

$$\left|\Psi_f(\alpha,\phi)\right\rangle = \cos\alpha\Big(\frac{1}{\sqrt{2}}(|H\rangle_s + e^{i\phi}|V\rangle_s)\Big)|H\rangle_a$$

(2.119)

$$+ e^{i\phi/2}\sin\alpha\Big(\cos\frac{\phi}{2}|H\rangle_s - i\sin\frac{\phi}{2}|V\rangle_s\Big)|V\rangle_a$$

We obtain the same result as with Equation 2.113, except Equation 2.119 gives the global state of the system based on polarization instead of the spatial mode. We may observe the wave properties of a photon by using polarization- and mode-based states. The last PBS is used to create a mode degeneracy again correlated with polarizations for detection. We find the intensity at detector D_0 as

(2.120)
$$I_0(\alpha,\phi) = \frac{1}{2}\cos^2\alpha + \cos^2\frac{\phi}{2}\sin^2\alpha,$$

which is the same as Equation 2.114, while again $I_1 = 1 - I_0$.

The most sophisticated component of the optical circuit is the c-Had gate which acts on a two-qubit state. The realization of this gate has been demonstrated in QDCE, which transforms the mode-based photonic states (Ionicioiu & Terno, 2011). The
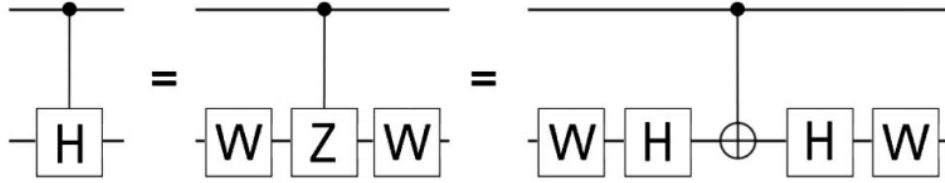
Figure 2.21 The c-Had gate. The c-Had is composed of a cZ gate and two W gates as in the order shown in the figure, where a cZ gate is composed of two Hadamard gates and a cNOT gate.

c-Had consists of several tools, as shown in Figure 2.21. We use a pol-based c-Had, which has been used to construct W-state-based quantum networks (Yesilyurt et al., 2016). The Hadamard gates can be realized by using HWPs at an angle of $\pi/8$, and we can realize W gates with HWPs at an angle of $\pi/16$. There are also experimental and theoretical works for the realization of an optical cNOT gate (Clark et al., 2009; Nemoto & Munro, 2004). A pair of photons can be emitted at 808 nm via parametric down-conversion (Peruzzo et al., 2012).

2.6.2.2 Some Applications of the c-Had Gate

In this subsection, we will discuss some works regarding the practical use of the c-Had gate. This will give an idea of how this quantum gate is essential and what it is capable of. We will introduce optical quantum circuits where one aims to generate W-state-based quantum networks.

The first work we introduce is about the expansion of W states whose entanglement is unique (Yesilyurt et al., 2016), and this type of states is a convenient choice for information processing tasks due to its robustness against environmental effects. The general expression for a W state is given as:

$$(2.121) \qquad |W_n\rangle = \frac{1}{\sqrt{n}}[|(n-1)_H\rangle_a|1_V\rangle_1 + \sqrt{n-1}|W_{n-1}\rangle_a|1_H\rangle_1].$$

In this proposal, the authors aim to obtain a W state whose size is twice as much; in other words, they aim to construct a circuit that transforms the input W state as follows:

$$(2.122) \qquad\qquad |W_n\rangle \longrightarrow |W_{2n}\rangle$$

where n is the number of qubits belonging to a W state. We will not get into details

on each transformation step, but one can see the expansion of a Bell state in Figure 2.22. This is the most basic expansion because one simply expands a Bell state given in the following:

$$(2.123) \qquad\qquad |W_2\rangle = \frac{1}{\sqrt{2}}(|HV\rangle + |VH\rangle),$$

and creates a W state of four photons. The whole process can be summarized as in the following:

$$(2.124) \qquad\qquad E\,|W_2\rangle = |W_4\rangle$$

where

$$(2.125) \qquad |W_4\rangle = \frac{1}{\sqrt{4}}(|HHHV\rangle + |HHVH\rangle + |HVHH\rangle + |VHHH\rangle).$$

The operator of the whole circuit, composed of 2 c-Had and two cNOT gates, is denoted by E. As a result, one doubles the size of the initial Bell state. If one repeats the same process to double the size of the four-photon W state, 8 two-qubit gates and 4 independent photons are required. The size of the circuit is as twice as the first circuit given in Figure 2.22. For expanding an n-qubit W state into a 2n-qubit W state, the number of required two-qubit gates is $2n$.

The other proposal we would like to discuss is about the construction of W states; however, in this work one generates a W state with arbitrary size starting from independent photons (Diker, 2022). It means that one does not need any entanglement among photons.

Initially, we start with three independent photons and transform their polarization states as in the previous case. The first circuit for creating a three-photon W state is shown in Figure 2.23. We have two $cNOT$ gates and two F gates. The input photon in mode 1 is polarized vertically, whereas the others are in the horizontally-polarized state. Each spatial mode is in the order starting from left to right in each ket. The transformations of the F gates in different colors are different. The black F gate can be decomposed into half-wave plates HWPs with an angle of $\pi/8$ and is the usual c-Had gate. We call these gates F to generalize for all angles. The quantum gates act on different qubits; therefore, two subindices are used to show the spatial modes
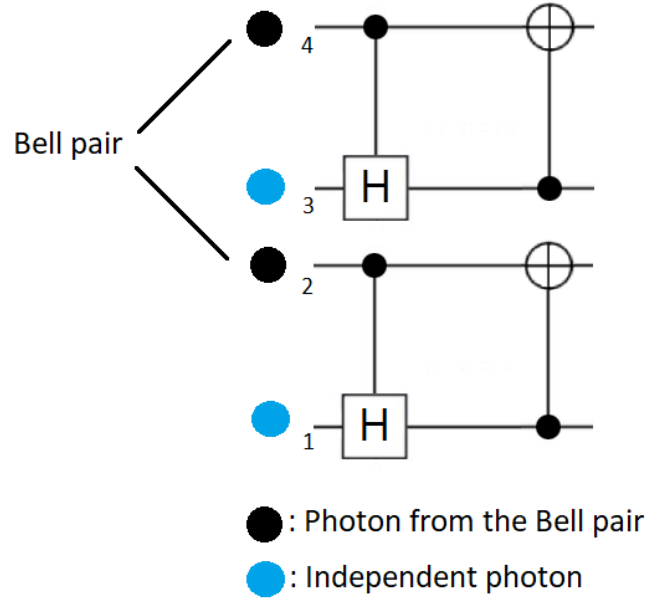
Figure 2.22 The quantum circuit for the generation of a four-qubit W state. One accesses each qubit of the Bell state (solid black spheres) and make them interact with independent photons (solid blue spheres). Thus, independent photons become entangled with the ones of the Bell state, and we obtain a W-state of four qubits as an output.

of the control and target qubit. Each step of the whole operation is as follows:

$$F_{23}cNOT_{21}F_{12}|VHH\rangle = F_{23}cNOT_{21}[|V\rangle \otimes (\frac{1}{\sqrt{3}}|H\rangle + \sqrt{\frac{2}{3}}|V\rangle) \otimes |H\rangle]$$

(2.126)

$$= F_{23}cNOT_{21}[\frac{1}{\sqrt{3}}|VHH\rangle + \sqrt{\frac{2}{3}}|VVH\rangle]$$

$$= F_{23}[\frac{1}{\sqrt{3}}|VHH\rangle + \sqrt{\frac{2}{3}}|HVH\rangle]$$

$$= \frac{1}{\sqrt{3}}(|VHH\rangle + |HVH\rangle + |HVV\rangle).$$

Finally, the last gate acting on our state is the $cNOT$ gate and gives a W state of three qubits as output,

(2.127)

$$cNOT_{32}[\frac{1}{\sqrt{3}}(|VHH\rangle + |HVH\rangle + |HVV\rangle)]$$

$$= \frac{1}{\sqrt{3}}(|VHH\rangle + |HVH\rangle + |HHV\rangle).$$

In the second circuit, four photons are used to create a W state with four qubits. The circuit is composed of five $cNOT$s and three F gates (Figure 2.24). The whole
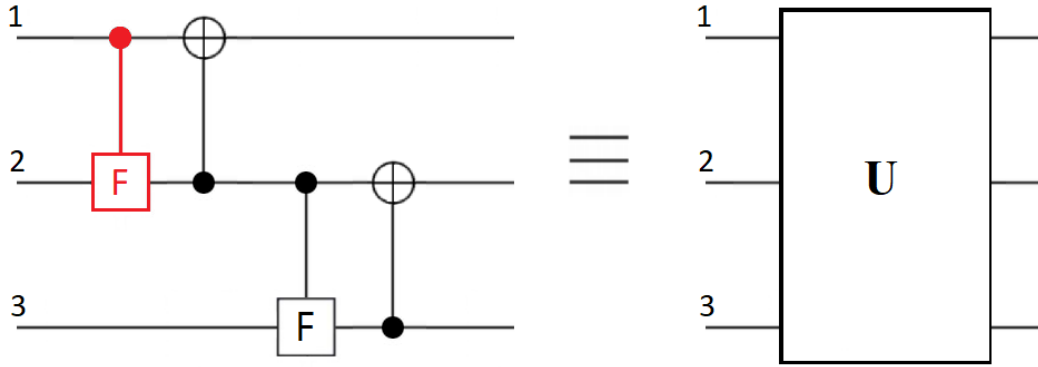
Figure 2.23 We send three photons into the circuit composed of two $cNOT$ gates and two F gates. All the gates correspond to the box U. The input state is $|VHH\rangle$, and, in the end, a W state of three qubits is obtained as output.

operator is shown as the U box (Figure 2.23). The U box acts on the photons as in the following:

$$(2.128) \qquad U|VHH\rangle = |W_3\rangle,$$

and $|W_3\rangle$ is a three-photon W state. One can see the operations of each gate in the following:

$$(2.129) \qquad F_{12}|VHHH\rangle = \frac{1}{\sqrt{4}}|VHHH\rangle + \sqrt{\frac{3}{4}}|VVHH\rangle.$$

U box transforms the second qubit of the resultant state because the photon's state
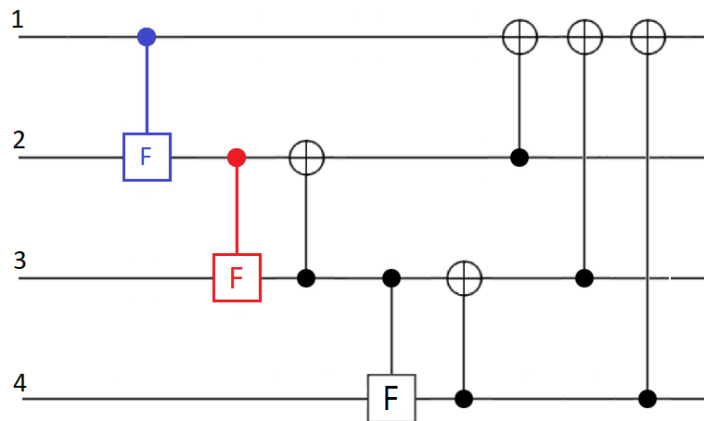
Figure 2.24 The enhanced optical scheme. This circuit consists of eight two-qubit gates, five of which are $cNOT$s. The other ones are F gates. We send four photons into the circuit to obtain a four-qubit W state.
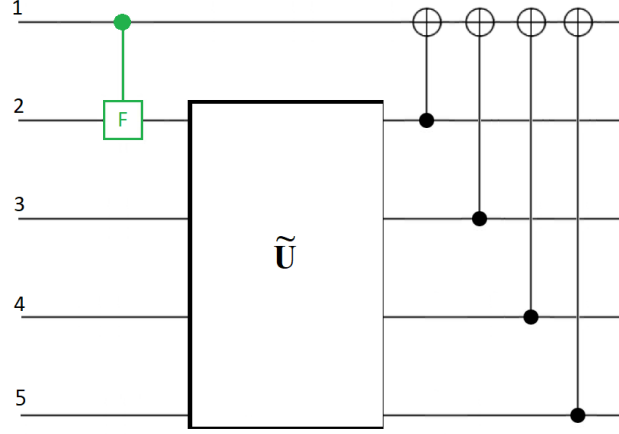
Figure 2.25 The optical circuit for the generation of a five-qubit W state. This circuit consists of a F gate, four $cNOT$ gates, and $\tilde{U}$ corresponding to the generation circuit for a 4-qubit W state. We add extra gates to the previous circuit, $\tilde{U}$, whose number is equal to the size of the resultant state.

is $|V\rangle$ in mode 2,

$$UF_{12}|VHHH\rangle = U\left[|V\rangle \otimes \left(\frac{1}{\sqrt{4}}|HHH\rangle + \sqrt{\frac{3}{4}}|VHH\rangle\right)\right]$$

(2.130)

$$= |V\rangle \otimes \left(\frac{1}{\sqrt{4}}|HHH\rangle + \sqrt{\frac{3}{4}}|W_3\rangle\right)$$

$$= \frac{1}{\sqrt{4}}(|VHHH\rangle + |VVHH\rangle + |VHVH\rangle + |VHHV\rangle).$$

After the action of the last three $cNOT$ gates, we obtain a W state of four photons:

(2.131)

$$cNOT_{21}cNOT_{31}cNOT_{41}[\frac{1}{\sqrt{4}}(|VHHH\rangle + |VVHH\rangle + |VHVH\rangle + |VHHV\rangle)]$$

$$= cNOT_{21}cNOT_{31}[\frac{1}{\sqrt{4}}(|VHHH\rangle + |VVHH\rangle + |VHVH\rangle + |HHHV\rangle)]$$

$$= cNOT_{21}[\frac{1}{\sqrt{4}}(|VHHH\rangle + |VVHH\rangle + |HHVH\rangle + |HHHV\rangle)]$$

$$= \frac{1}{\sqrt{4}}(|VHHH\rangle + |HVHH\rangle + |HHVH\rangle + |HHHV\rangle)$$

$$= |W_4\rangle.$$

One can generate a W state of five qubits by using an ancillary photon. The corresponding circuit is shown in Figure 2.25. The previous network, which can be used to generate a four-qubit W state, is denoted by $\tilde{U}$. The transformations of the

Table 2.2 The number of gates required for the generation of W states.

Resultant W state	Two-qubit gates used	F gates	$cNOT$ gates
$|W_3\rangle$	4	2	2
$|W_4\rangle$	8	3	5
$|W_5\rangle$	13	4	9
$|W_6\rangle$	19	5	14
$|W_7\rangle$	26	6	20

initially independent photons are given below:

$$(2.132) \qquad \tilde{U}F_{12}|VHHHH\rangle = \frac{1}{\sqrt{5}}|VHHHH\rangle + \sqrt{\frac{4}{5}}|V\rangle \otimes |W_4\rangle,$$

(2.133)

$$cNOT_{21}cNOT_{31}cNOT_{41}cNOT_{51}\tilde{U}F_{12}|VHHHH\rangle$$

$$= cNOT_{21}cNOT_{31}cNOT_{41}cNOT_{51}\left[\frac{1}{\sqrt{5}}|VHHHH\rangle + \sqrt{\frac{4}{5}}|V\rangle \otimes |W_4\rangle\right]$$

$$= \frac{1}{\sqrt{5}}(|VHHHH\rangle + |HVHHH\rangle + |HHVHH\rangle + |HHHVH\rangle + |HHHHV\rangle)$$

$$= |W_5\rangle.$$

Three circuits have been shown, and the total number of required two-qubit gates are 4, 8, and 13 to obtain three-, four- and five-qubit W states, respectively. When one wants to enlarge the size of a W state by one qubit, n two-qubit gates must be integrated into the circuit which generates the initial W state (n is the number of qubits of the desired W state). This shows a pattern for the number of gates required for each W state, and we obtain

$$(2.134) \qquad \frac{n(n+1)-4}{2}$$

which gives the number of required two-qubit gates. The number of F gates we need

$$(2.135) \qquad n-1,$$

and the number of $cNOT$ gates is given as

$$(2.136) \qquad \frac{(n-2)(n+1)}{2}.$$

For the generation of an n-qubit W state, we need $n-1$ F gates with transformations
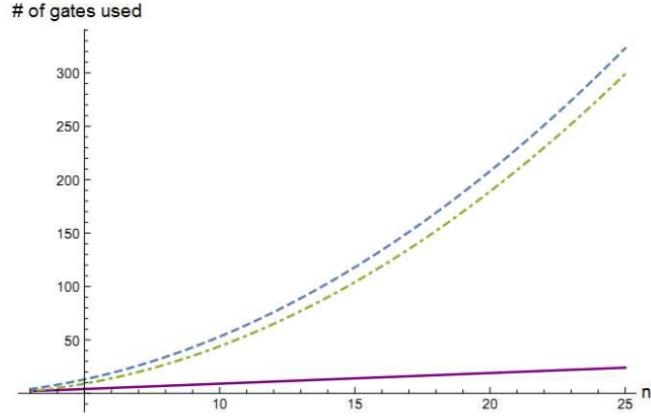
Figure 2.26 The blue dashed line shows the relation between the number of qubits and the total number of two-qubit gates. The green dashed-dotted line shows the relation between n (the number of qubits of W state) and the number of $cNOT$ gates. The solid purple line shows the relation between the number of F gates and n.

given in the following:

$$F_{(n-1)n}|10\rangle = |1\rangle \otimes \frac{1}{\sqrt{2}}(|0\rangle + |1\rangle),$$
$$F_{(n-2)(n-1)}|10\rangle = |1\rangle \otimes (\frac{1}{\sqrt{3}}|0\rangle + \sqrt{\frac{2}{3}}|1\rangle),$$

.

(2.137)   .

.

$$F_{23}|10\rangle = |1\rangle \otimes (\frac{1}{\sqrt{n-1}}|0\rangle + \sqrt{\frac{n-2}{n-1}}|1\rangle),$$
$$F_{12}|10\rangle = |1\rangle \otimes (\frac{1}{\sqrt{n}}|0\rangle + \sqrt{\frac{n-1}{n}}|1\rangle)$$

where the subindices give the modes of qubits. The first and the second indices are the modes of the control and target qubits, respectively. One can check Table 2.2 on which we show the number of gates needed for the generation of certain W states. The number of two-qubit gates required to generate an n-qubit W state is proportional to n^2, which means a quadratic increase. We give the graph between the total number of $cNOT$s and the size of the resultant W state in Figure 2.26. We provide the graph between the angle of the first HWP and the size of the obtained W state in Figure 2.27. We see that

(2.138) $$\theta = \frac{1}{4}\arccos[\frac{1}{\sqrt{n}}].$$

Three optical setups have been proposed, which create W states of three, four, and

68

five qubits with unit probability (not considering the application probabilities of the quantum gates). A W state of any size can be generated by integrating extra gates into the initial circuit. We have also found the formula which gives the number of gates required. Our proposal is capable of creating any W state, and the number of gates depends on the size of the W state to be obtained. Also, we only use cZ and $cNOT$ gates and do not need any larger gate. The realization of the $cNOT$ gate has been shown in the literature.

2.6.2.3 Entanglement in the Quantum Delayed-Choice Experiment

As mentioned earlier, the QDCE has been demonstrated to show that photons may reveal both the particle and wave properties simultaneously. In this experiment, a two-photon state is transformed by quantum gates in the optical scheme. Recall that the essential component of the circuit is the c-Had gate (a two-qubit quantum gate). We have already discussed how it transforms states and how to realize it using mode- and polarization-based methods. One uses entangled two-photon states to observe the wave- and particle-like properties through its intensity. We use the c-Had gate
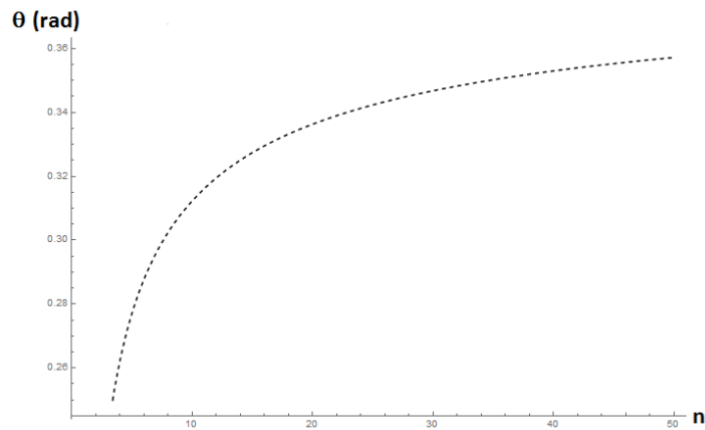
Figure 2.27 A graph of the relation between the orientation angle of the first HWP and the number of qubits belonging to the resultant W state. The other HWPs act on the qubits as shown in Eq.2.137. The relation between n and the angles of the other HWPs is also shown in the graph. This graph guides us how to arrange our HWPs such that the circuit creates an n-qubit W state.

to entangle two photons. Let us recall the resultant state:

$$\left|\Psi_f(\alpha,\phi)\right\rangle = \cos\alpha\Big(\frac{1}{\sqrt{2}}(|0\rangle_s + e^{i\phi}|1\rangle_s)\Big)|0\rangle_a$$
$$+ \sin\alpha\Big(\cos\frac{\phi}{2}|0\rangle_s - i\sin\frac{\phi}{2}|1\rangle_s\Big)|1\rangle_a,$$

which was given previously. By measuring the intensity of the system photon, we get

$$I_0(\alpha,\phi) = \frac{1}{2}\cos^2\alpha + \cos^2\frac{\phi}{2}\sin^2\alpha.$$

We will investigate this experiment from the point of entanglement (Diker, 2021). The general concurrence expression is given as

$$(2.139) \qquad\qquad C(\phi) = \left\langle\phi\middle|\tilde{\phi}\right\rangle$$

for two-qubit states (Wootters, 2001). We simply apply this to the global state of two photons (Diker, 2021) and get

$$(2.140) \qquad\qquad C(\alpha,\phi) = \frac{1}{\sqrt{2}}(|\sin 2\alpha|\sqrt{1+\sin^2\phi}).$$

Concurrence depends on both the relative phase and the amplitude, which implies a correlation between concurrence (the measure of entanglement) and the probability of observing the system photon. Concurrence and intensity can be expressed in terms of each other (together with α and ϕ). Using this fact, we find the equation,

$$(2.141) \qquad\qquad I_0(\alpha,\phi) = \frac{1}{2}\Big(\cos^2\alpha + \cos^2\frac{\phi}{2}\frac{C(\alpha,\phi)^2}{\cos^2\alpha(1+\sin^2\phi)}\Big).$$

The intensity equation and concurrence are correlated with each other through the parameters α and ϕ (Diker, 2021). One should notice that concurrence and other trigonometric terms are also correlated with each other as well; because concurrence and intensity depend on the same parameters. We observe not only particle and wave behaviors but also the entanglement between the photons (Diker, 2021). Equation 2.141 gives the direct correlation between entanglement and intensity. The c-Had gate is the main component which entangles photons.

2.6.2.4 Quantum Contextuality in The Delayed-Choice Experiment

The importance of the KCBS inequality comes from the fact that it is the simplest non-contextuality inequality. Let us recall the KCBS scenario which is a five-measurement non-contextuality inequality (Klyachko, 2002, 2007; Binicioğlu et al., 2007; Klyachko et al., 2008):

$$\langle A_1 A_2 \rangle + \langle A_2 A_3 \rangle + \langle A_3 A_4 \rangle + \langle A_4 A_5 \rangle + \langle A_5 A_1 \rangle \geq -3$$

where $A_i = 2S_i^2 - 1$. (S_i are the 3×3 spin-1 matrices). In real space, one may find five directions for spin measurements performed on qutrit states. A_i and A_{i+1} are compatible observables. It means that one may measure them together. Recall that the quantum lower limit can be as low as $\cong -3,94$ for the neutrally polarized spin state $|0\rangle$.

Contextuality is an intrinsically defined feature for qutrit states; in other words, one does not need to take into account the spatial parameters. Nevertheless, a qutrit can have self-entanglement (Can et al., 2005) which can be defined as an embedded entanglement in a qutrit system. The symmetric subgroup of two-qubit states, which corresponds to effective qutrits, has been investigated. One finds the concurrence inequality as a measure of self-entanglement (Binicioğlu et al., 2007). We will discuss an optical scheme where the symmetric two-qubit states are used as input and show the direct relation between the wave-particle duality and quantum contextuality (Diker, view). Along this direction, we will discuss how the KCBS test is applied, and which operators we will need.

As mentioned earlier, the symmetric two-qubit states are inputs because they correspond to effective qutrits on which one performs the KCBS measurements. The most general symmetric expression of two-qubit states is given as:

$$(2.142) \qquad |\Psi\rangle = \boldsymbol{\alpha_1}|00\rangle + \boldsymbol{\beta}\left(\frac{|01\rangle + |10\rangle}{\sqrt{2}}\right) + \boldsymbol{\alpha_2}|11\rangle$$

where $\boldsymbol{\alpha_1}$ and $\boldsymbol{\alpha_2}$ are taken as equal,

$$(2.143) \qquad \boldsymbol{\alpha_1} = \boldsymbol{\alpha_2} = \alpha e^{i\gamma}, \;\; \boldsymbol{\beta} = \beta e^{\eta}.$$

The phase difference between the probability amplitudes is $\eta - \gamma = \phi$. Equation 2.142 gives the initial state put into our circuit. Then, consecutive gates act on this state before we perform the final test. This test includes the KCBS measurements performed on both qubits along the vectors seen in Figure 2.1. The optical circuit

is composed of a cZ gate, a cNOT gate, and a Hadamard gate. Finally, the KCBS measurements are performed. Qubits physically correspond to spin-1/2 particles. Recall that the cNOT gate transforms a quantum state only when the control qubit is in the $|1\rangle$ state corresponding to a particle with $-\frac{1}{2}$ spin. The state of the target qubit is changed from $|0\rangle$ to $|1\rangle$, or $|1\rangle$ to $|0\rangle$. A Hadamard gate is applied onto the second qubit as follows: $H|0\rangle = 1/\sqrt{2}(|0\rangle + |1\rangle)$, and $H|1\rangle = 1/\sqrt{2}(|0\rangle - |1\rangle)$. The cZ gate is a two-qubit gate whose transformation is given as:

$$(2.144) \qquad\qquad cZ|11\rangle = -|11\rangle$$

while all other states remain unchanged. One can see the whole circuit in Figure 2.28. Let us look at each step of transformation performed by each gate. The first one is the Hadamard gate which acts on the initial state as follows:

$$(I \otimes H)|\Psi\rangle = \frac{\boldsymbol{\alpha_1}}{\sqrt{2}}|0\rangle \otimes (|0\rangle + |1\rangle)$$

$$(2.145) \qquad + \frac{\boldsymbol{\beta}}{\sqrt{2}}\left(|0\rangle \otimes \frac{1}{\sqrt{2}}(|0\rangle - |1\rangle) + |1\rangle \otimes \frac{1}{\sqrt{2}}(|0\rangle + |1\rangle)\right)$$

$$+ \frac{\boldsymbol{\alpha_2}}{\sqrt{2}}|1\rangle \otimes (|0\rangle - |1\rangle).$$

Next, the cZ gate transforms the state in Equation 2.145 as in the following:

$$cZ(I \otimes H)|\Psi\rangle = \frac{\boldsymbol{\alpha_1}}{\sqrt{2}}|0\rangle \otimes (|0\rangle + |1\rangle)$$

$$(2.146) \qquad + \frac{\boldsymbol{\beta}}{\sqrt{2}}\left(|0\rangle \otimes \frac{1}{\sqrt{2}}(|0\rangle - |1\rangle) + |1\rangle \otimes \frac{1}{\sqrt{2}}(|0\rangle - |1\rangle)\right)$$

$$+ \frac{\boldsymbol{\alpha_2}}{\sqrt{2}}|1\rangle \otimes (|0\rangle + |1\rangle).$$

The last gate we use is the cNOT gate which gives the final state as follows:

$$cNOT_{12}cZ(I \otimes H)|\Psi\rangle = \frac{\alpha}{\sqrt{2}} + \frac{\beta e^{i\phi}}{2}|00\rangle + \frac{\alpha}{\sqrt{2}} - \frac{\beta e^{i\phi}}{2}|01\rangle$$

$$(2.147)$$

$$+ \frac{\alpha}{\sqrt{2}} - \frac{\beta e^{i\phi}}{2}|10\rangle + \frac{\alpha}{\sqrt{2}} + \frac{\beta e^{i\phi}}{2}|11\rangle.$$

We have specifically chosen these gates to keep the symmetry of the final form. Thus, the final expression of the two-qubit state given in Equation 2.147 corresponds to an effective qutrit (three-level quantum system). We can rewrite it as

$$(2.148) \qquad |\Psi^*\rangle = \frac{\alpha}{\sqrt{2}} + \frac{\beta e^{i\phi}}{2}|1\rangle + \alpha - \frac{\beta e^{i\phi}}{\sqrt{2}}|0\rangle + \frac{\alpha}{\sqrt{2}} + \frac{\beta e^{i\phi}}{2}|-1\rangle.$$

The KCBS Test
(Spin Measurement)
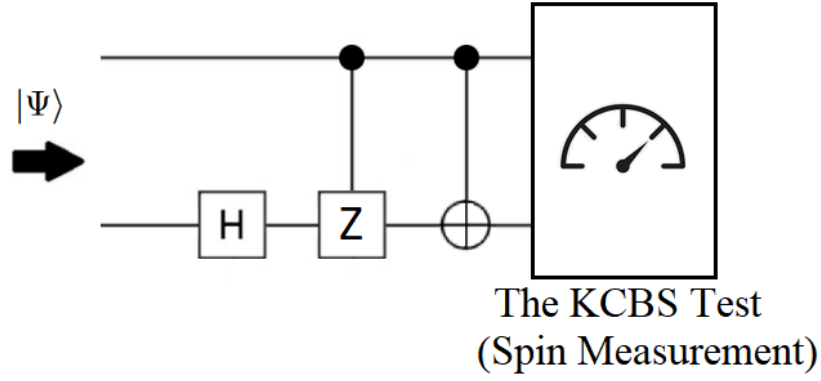
Figure 2.28 The circuit consists of 2 two-qubit gates(a cZ and a cNOT gates) and a Hadamard gate. In the end, the total spin of two spin-1/2 particles is measured, which corresponds to a spin measurement of a spin-1 particle.

We use the normalization condition,

(2.149)
$$2\alpha^2 + \beta^2 = 1$$

to rewrite α and β as below:

(2.150)
$$\alpha = \frac{\cos\theta}{\sqrt{2}}, \beta = \sin\theta.$$

This allows us to write the state as a function of ϕ and θ, $|\Psi^*(\theta,\phi)\rangle$. Finally, we test it by performing the KCBS measurements. The operation of the KCBS test is denoted by S_{KCBS}. We calculate the average of the KCBS operator and get

(2.151)
$$\langle\Psi^*|S_{KCBS}|\Psi^*\rangle = -\left(3\sqrt{5}-5\right)\left(\cos^2\theta - \sin 2\theta\cos\phi\right) - \sqrt{5}$$

Equation 2.151 depends on both θ and ϕ; in other words, quantum contextuality depends on the wave- and particle-like features (Diker, view). It is known that a subgroup of qutrits violates the KCBS inequality (Klyachko, 2002, 2007; Binicioğlu et al., 2007; Klyachko et al., 2008). Yet, the degree of violation changes from state to state. We observe maximal contextuality for the state $|0\rangle$. Through Equation 2.151, one can clearly find the quantum lower limit when

(2.152)
$$\cos^2\theta - \sin 2\theta\cos\phi = 1.$$

 We have the θ variable corresponding to the particle property of the photon, whereas ϕ is the initial relative phase between the amplitudes. It is trivial to say that this is the wave nature of the photon. The probability amplitude of the state

$|0\rangle$ given in Equation 2.148 is dependent on β, α and ϕ. The α parameter expresses the particle interaction when the gates act on both photons. Both α and β depend on θ; therefore, the θ parameter corresponds to the particle nature of photons. A two-qubit system exhibits wave- and particle-like properties such that The KCBS inequality is maximally violated; in other words, both particles exhibit these properties in accordance with the maximal contextuality (Diker, view). Let us say $\phi = \frac{\pi}{2}$, the KCBS inequality is maximally violated for $\theta = n\pi$ (n is an integer). If one increases the phase difference from $\frac{\pi}{2}$ to π, the violation is maximal when $\theta \in \{\tan^{-1}(2), \pi, \tan^{-1}(2) - \pi, 2\pi\}$.

3. CONCLUSION

The KCBS inequality is the simple and elegant example of KS-like inequalities. Therefore, we did the rotational-symmetry analysis of the KCBS scenario. We have seen its symmetry about the Z-axis and found the contextuality region for the neutrally-polarized state, which maximally violates the KCBS inequality. The other eigenstates of the spin-1 measurement operator have also been investigated, and it has been shown that they exhibit non-contextuality without regard to rotation. Yet, their homogeneous linear combination exhibit contextuality in the KCBS scenario.

The specific set of qutrits with real probability amplitudes (retrits) have been investigated. By doing a graph analysis, we have determined the set of contextual retrits through physical rotations. The (non-)contextuality regions have been shown on spheres. Furthermore, the set of rotation angles has been found for which no contextuality is observed, i.e., the set of KCBS measurements yielding results compatible with the classical approach have been determined.

The data have been provided for specific Euler angles giving maximal contextuality. Data points have been shown on graphs, and we have fitted the corresponding curve to find general formulas. This sets the condition for a state to be maximally contextual. This is an important step towards the classification of quantum systems in terms of their (non-)contextuality.

After we have analyzed quantum contextuality regarding its symmetry in the physical space, we have decided to determine the degree of contextuality for the symmetric subgroup of two-qubit states expressed in MSR. Later, a connection between contextuality and concurrence has been found in Equation 2.93. We have made use of this relation to find the maximal quantum contextuality when concurrence (the measure of entanglement) is given. We have found a linear relation between the measure of entanglement and contextuality. We have also checked the non-entanglement and maximal entanglement cases, which give us the quantum and the classical lower limits. These limits show that non-locality is necessary but insufficient for a qutrit to violate the non-contextuality inequality. They have to be non-local as well to

observe the violation of the KCBS inequality. These conditions have been shown in (Klyachko, 2007; Klyachko et al., 2008), and the authors have already shown the correlation between the degree of entanglement and contextuality. We succeeded in showing this correlation explicitly. The qutrit states can be divided into three groups:

i. The qutrits which never exhibit contextuality in the KCBS scenario;

ii. The states which exhibit contextuality in the KCBS scenario to a certain degree (not maximally);

iii. The maximally contextual states that yield the quantum lower limit.

Subcategories may be added to divide qutrits into:

i. non-local and contextual states for $S < -3$;

ii. Those that exhibit non-contextuality and non-locality $(-3 \leq S < -\sqrt{5})$;

iii. Those that exhibit non-contextuality and locality $(-\sqrt{5} \leq S)$.

We use the relation between concurrence and contextuality to determine these categories. One can use the results in (Soeda et al., 2013) based on the relation between the CHSH and KCBS inequalities to categorize qutrits in a similar manner. Categorization of qutrit states based on their contextuality and entanglement is required for a better understanding of these concepts. Moreover, we chose the KCBS scenario for this purpose because it is the simplest example of a classical inequality.

After we investigated the symmetries of the KCBS scenario and how its violation is related to entanglement, we have looked into the delayed-choice experiment in the context of contextuality. We have seen that the QDCE can be demonstrated by using a polarization-based optical circuit and how the wave- and particle-like properties are related to the degree of entanglement in a two-photon system. The QDCE has already been proposed using polarization-based photons (Diker, 2018); however, our scheme is composed of fewer optical tools. We have used a polarization-based c-Had not to require an entanglement source since it entangles the photonic states. The QDCE has been realized via various methods, including single-atom protocol and nuclear magnetic resonance techniques (Manning et al., 2015; Roy et al., 2012; Tang et al., 2012). Lately, entanglement-assisted QDCEs have been discussed, and the hidden-variable models have been considered as to whether they are in agreement with the results (Ionicioiu et al., 2014; Xin et al., 2015). The polarization-based scheme is yet to be demonstrated experimentally; however, one can realize the cNOT gate via linear optics, and the other tools are easy to find in

laboratories.

It has been shown that the wave-particle duality and entanglement may be observed simultaneously through the intensity of a photon. Two unique concepts of quantumness: entanglement and the wave-particle duality can be observed simultaneously due to their strong correlation in the QDCE. One may generate entanglement between the particle and wave states in a two-photon state (Rab et al., 2017); however, entanglement (together with the wave-particle duality) can be observed in the QDCE. The QDCE has also been demonstrated in a multi-path scheme, which uses control-Hadamard gates (Chen et al., 2021). There is an open problem as to whether one may observe entanglement and the wave-particle duality simultaneously in a generalized scenario. Our results are important to understand the connection between the wave-particle duality and entanglement.

In the context of the QDCE, we have proposed a quantum circuit that is the modified QDCE and seen that quantum contextuality and the wave-particle duality are correlated with each other in a two-qubit system. We have obtained the equation showing the direct relation between these. This proposal is realizable since we use well-known tools. Our result is essential to understand the fundamental properties of Quantum Theory. The KCBS inequality was a good choice to look for possible relations between these fundamental concepts due to its simplicity.

Finally, we are ready to manifest the physical reality of quantum contextuality. Let us look at the following fundamental properties concerning the role of quantum contextuality in Quantum Theory:

i. There is not a generalized monogamy relation between non-locality and quantum contextuality; in other words: observing one or another depends on the measurements, but it cannot be generalized to any case (Xiao et al., 2022).

ii. There is a rotational symmetry of quantum contextuality in the KCBS measurement scenario, which is likely to be valid for other measurement scenarios as well.

iii. Entanglement and quantum contextuality are linearly related in the KCBS scenario.

iv. The lower bound we have found $(-\sqrt{5})$ is the stricter separation between classical and quantum measurements. We have drawn a more precise line between quantum and classical worlds and stepped towards understanding quantum dynamics better.

v. Quantum contextuality is as strongly correlated with entanglement as with

the wave-particle duality. Entanglement is also well correlated with the wave and particle properties of a particle.

BIBLIOGRAPHY

Ahrens, J., Amselem, E., Cabello, A., & Bourennane, M. (2013). Two fundamental experimental tests of nonclassicality with qutrits. *Scientific Reports*, *3*, 1.

Aravind, P. K. (2017). Mubs and sic-povms of a spin-1 system from the majorana approach. Preprint at https://arxiv.org/abs/1707.02601.

Aspect, A., Dalibard, J., & Roger, G. (1982). Experimental test of bell's inequalities using time-varying analyzers. *Physical Review Letters*, *49*, 1804.

Bell, J. S. (1964). On the einstein podolsky rosen paradox. *Physics*, *1*, 195.

Bell, J. S. (1966). On the problem of hidden variables in quantum mechanics. *Reviews of Modern physics*, *38*, 447.

Binicioğlu, S., Can, M. A., Klyachko, A. A., & Shumovsky, A. S. (2007). Entanglement of a single spin-1 object: an example of ubiquitous entanglement. *Foundations of Physics*, *37*, 1253–1277.

Bloch, F. & Rabi, I. I. (1945). Atoms in variable magnetic fields. *Reviews of Modern Physics*, *17*, 237.

Budroni, C., Cabello, A., Gühne, O., Kleinmann, M., & Larsson, J. (2022). Kochenspecker contextuality. Preprint at https://arxiv.org/abs/2102.13036.

Cabello, A., Amselem, E., Blanchfield, K., Bourennane, M., & Bengtsson, I. (2012). Proposed experiments of qutrit state-independent contextuality and two-qutrit contextuality-based nonlocality. *Physical Review A*, *85(3)*, 032108.

Can, M. A., Klyachko, A. A., & Shumovsky, A. S. (2005). Single-particle entanglement. *Journal of Optics B: Quantum and Semiclassical Optics*, *7*, L1.

Chen, Y., Nie, F., Xie, S.-Q., Zheng, Y.-F., Dai, Q., Bray, T., Wang, Y.-X., Xing, J.-F., Huang, Z.-J., Wang, D.-P., et al. (2021). Efficient assembly of nanopore reads via highly accurate and intact error correction. *Nature Communications*, *12(1)*, 1–10.

Clark, A. S., Fulconis, J., Rarity, J. G., Wadsworth, W. J., & O'Brien, J. L. (2009). All-optical-fiber polarization-based quantum logic gate. *Physical Review A*, *79(3)*, 030303.

Clauser, J. F., Horne, M. A., Shimony, A., & Holt, R. A. (1969). Proposed experiment to test local hidden-variable theories. *Physical Review Letters*, *23*, 880.

Diker, F. (2018). Quantum delayed-choice protocol by means of the polarization degree of freedom of a photon. *Journal of the Optical Society of America B*, *35(2)*, 284–286.

Diker, F. (2021). Mathematical relation between concurrence and intensity of a photon in the quantum delayed-choice experiment. In *Journal of Physics: Conference Series*, volume 2148, (pp. 012010). IOP Publishing.

Diker, F. (2022). Deterministic construction of arbitrary w states with quadratically increasing number of two-qubit gates. Preprint at https://arxiv.org/abs/1606.09290v3.

Diker, F. (Under Review). Quantum contextuality is in good agreement with the delayed-choice method. -, -, −.

Diker, F. & Gedik, Z. Retrit states violating the kcbs inequality and necessary conditions for maximal contextuality. In *IC-MSQUARE 2022 Proceedings*. (Accepted for publication) AIP Publishing.

Diker, F. & Gedik, Z. (2022). The degree of quantum contextuality in terms of concurrence for the kcbs scenario. *International Journal of Theoretical Physics*, *61*, 266.

Dirac, P. A. M. (1958). *Quantum Mechanics* (4th ed.). London: Oxford University Press.

Einstein, A., Podolsky, B., & Rosen, N. (1935). Can quantum-mechanical description of physical reality be considered complete? *Physical review*, *47(10)*, 777.

Englert, B.-G. (1996). Fringe visibility and which-way information: An inequality. *Physical Review Letters*, *77(11)*, 2154.

Feynman, R. P., Leighton, R. B., & Sands, M. L. (1965). *Lecture Notes on Physics vol. III*. Boston: Addison-Wesley.

Freedman, S. J. & Clauser, J. F. (1972). Experimental test of local hidden-variable theories. *Physical Review Letters*, *28*, 938.

Gisin, N. (1991). Bell's inequality holds for all non-product states. *Physics Letters A*, *154*, 201–202.

Gleason, A. M. (1957). Measures on the closed subspaces of a hilbert space. *Journal of Mathematics and Mechanics*, *6*, 885–893.

Heisenberg, W. (1927). Über den anschaulichen Inhalt der quantentheoretischen Kinematik und Mechanik. *Zeitschrift für Physik*, *43*, 172.

Hellmuth, T., Walther, H., Zajonc, A., & Schleich, W. (1987). Delayed-choice experiments in quantum interference. *Physical Review A*, *35(6)*, 2532.

Herbert, N. & Karush, J. (1978). Generalization of bell's theorem. *Foundations of Physics*, *8(3)*, 313–317.

Heywood, P. & Redhead, M. L. G. (1983). Nonlocality and the kochen-specker paradox. *Foundations of physics*, *13(5)*, 481–499.

Hofmann, H. F. & Takeuchi, S. (2002). Quantum phase gate for photonic qubits using only beam splitters and postselection. *Physical Review A*, *66(2)*, 024308.

Ionicioiu, R., Jennewein, T., Mann, R. B., & Terno, D. R. (2014). Is wave–particle objectivity compatible with determinism and locality? *Nature Communications*, *5(1)*, 1–6.

Ionicioiu, R. & Terno, D. R. (2011). Proposal for a quantum delayed-choice experiment. *Physical Review Letters*, *107 (23)*, 230406.

Jacques, V., Wu, E., Grosshans, F., Treussart, F., Grangier, P., Aspect, A., & Roch, J.-F. (2007). Experimental realization of wheeler's delayed-choice gedanken experiment. *Science*, *315*, 966–968.

Kim, Y.-H., Yu, R., Kulik, S. P., Shih, Y., & Scully, M. O. (2000). Delayed "choice" quantum eraser. *Physical Review Letters*, *84(1)*, 1.

Klyachko, A. (2002). Coherent states, entanglement, and geometric invariant theory. Preprint at https://arxiv.org/abs/quant-ph/0206012.

Klyachko, A. (2007). Dynamical symmetry approach to entanglement. In J. P. Gazeau, J. Nešetřil, & B. Rovan (Eds.), *Physics and theoretical computer science: from numbers and languages to (quantum) cryptography security* (pp. 25–54). Amsterdam: Ios Press.

Klyachko, A. A., Can, M. A., Binicioğlu, S., & Shumovsky, A. S. (2008). Simple test for hidden variables in spin-1 systems. *Physical Review Letters*, *101*, 020403.

Kochen, S. & Specker, E. P. (1967). The problem of hidden variables in quantum mechanics. *Journal of Mathematics and Mechanics*, *17*, 59—-87.

Kurzyński, P., Cabello, A., & Kaszlikowski, D. (2014). Fundamental monogamy relation between contextuality and nonlocality. *Physical Review Letters*, *112(10)*, 100401.

Kurzyński, P. & Kaszlikowski, D. (2012). Contextuality of almost all qutrit states can be revealed with nine observables. *Physical Review A*, *86*, 042125.

Lawson-Daku, B. J., Asimov, R., Gorceix, O., Miniatura, C., Robert, J., & Baudon, J. (1996). Delayed choices in atom stern-gerlach interferometry. *Physical Review A*, *54(6)*, 5042.

Majorana, E. (1932). Atomi orientati in campo magnetico variabile. *Nuovo Cimento*, *9*, 43–50.

Manning, A. G., Khakimov, R. I., Dall, R. G., & Truscott, A. G. (2015). Wheeler's delayed-choice gedanken experiment with a single atom. *Nature Physics*, *11(7)*, 539–542.

Mäkelä, H. & Messina, A. (2010). N-qubit states as points on the bloch sphere. *Physica Scripta*, *140*, 014054.

Nemoto, K. & Munro, W. J. (2004). Nearly deterministic linear optical controlled-not gate. *Physical Review Letters*, *93(25)*, 250502.

Peruzzo, A., Shadbolt, P., Brunner, N., Popescu, S., & O'Brien, J. L. (2012). A quantum delayed-choice experiment. *Science*, *338 (6107)*, 634–637.

Rab, A. S., Polino, E., Man, Z. X., An, N. B., Xia, Y. J., Spagnolo, N., Franco, R. L., & Sciarrino, F. (2017). Entanglement of photons in their dual wave-particle nature. *Nature Communications*, *8(1)*, 1–7.

Ralph, T. C., Langford, N. K., Bell, T. B., & White, A. G. (2002). Linear optical controlled-not gate in the coincidence basis. *Physical Review A*, *65(6)*, 062324.

Roy, S. S., Shukla, A., & Mahesh, T. S. (2012). Nmr implementation of a quantum delayed-choice experiment. *Physical Review A*, *85(2)*, 022109.

Sakurai, J. J. & Napolitano, J. (2011). *Modern Quantum Mechanics* (2nd ed.). San Francisco: Pearson.

Scully, M. O., Englert, B.-G., & Walther, H. (1991). Quantum optical tests of complementarity. *Nature*, *351*, 111–116.

Soeda, A., Kurzyński, P., Ramanathan, R., Modi, K., & Kaszlikowski, D. (2013). Relation between nonlocality and contextuality for a biphoton. *Physical Review A*, *87(2)*, 022120.

Specker, E. P. (1960). Die logik nicht gleichzeitig entsc heidbarer aussagen. *Dialectica*, *14*, 239—-246.

Stapp, H. P. (1982). Bell's theorem as a nonlocality property of quantum theory. *Physical Review Letters*, *49(20)*, 1470.

Tang, J.-S., Li, Y.-L., Xu, X.-Y., Xiang, G.-Y., Li, C.-F., & Guo, G.-C. (2012). Realization of quantum wheeler's delayed-choice experiment. *Nature Photonics*, *6(9)*, 600–604.

Verstraete, F. & Wolf, M. M. (2002). Entanglement versus bell violations and their behavior under local filtering operations. *Physical Review Letters*, *89*, 170401.

Weizsäcker, K. F. (1931). Ortsbestimmung eines elektrons durch ein mikroskop. *Zeitschrift für Physik*, *70(1)*, 114–130.

Wheeler, J. A. (1978). The "past" and the "delayed-choice" double-slit experiment. In *Mathematical foundations of quantum theory* (pp. 9–48). Elsevier.

Wheeler, J. A., Zurek, W. H., & Ballentine, L. E. (1984). Quantum theory and measurement. *American Journal of Physics*, *52 (10)*, 955–955.

Wootters, W. K. (1998). Entanglement of formation of an arbitrary state of two qubits. *Physical Review Letters*, *80*, 2245.

Wootters, W. K. (2001). Entanglement of formation and concurrence. *Quantum Information and Computation*, *1*, 27–44.

Xiao, L., Ruffolo, G., Mazzari, A., Cunha, M. T., Rabelo, R., & Xue, P. (2022). Synchronous observation of bell nonlocality and state-dependent kochen-specker contextuality. Preprint at https://arxiv.org/abs/2204.05385.

Xin, T., Li, H., Wang, B.-X., & Long, G.-L. (2015). Realization of an entanglement-assisted quantum delayed-choice experiment. *Physical Review A*, *92(2)*, 022126.

Yesilyurt, C., Bugu, S., Ozaydin, F., Altintas, A. A., Tame, M., Yang, L., & Özdemir, Ş. K. (2016). Deterministic local doubling of w states. *Journal of the Optical Society of America B*, *33(11)*, 2313–2319.

Yu, S. & Oh, C. (2012). State-independent proof of kochen-specker theorem with 13 rays. *Phys. Rev. Lett.*, *108*, 030402.

Zeilinger, A., Weihs, G., Jennewein, T., & Aspelmeyer, M. (2005). Happy centenary, photon. *Nature*, *433*, 230–238.

Zhan, X., Zhang, X., Li, J., Zhang, Y., Sanders, B. C., & Xue, P. (2016). Realization of the contextuality-nonlocality tradeoff with a qubit-qutrit photon pair. *Physical Review Letters*, *116(9)*, 090401.

Łapkiewicz, R., Li, P., Schaeff, C., Langford, N., Ramelow, S., Wiésniak, M., & Zeilinger, A. (2011). Experimental non-classicality of an indivisible quantum system. *Nature*, *474*, 490–493.